Advanced Optics on Zinc Oxide

Bernard Gil

Laboratoire Charles Coulomb
CNRS - Université Montpellier 2

bgil@um2.fr

Outline

1- Cristallography, optical properties, basic concepts

2- Optical properties of heteroepitaxial polar ZnO-ZnMgO quantum wells

3- Optical properties of M-plane oriented nonpolar homoepitaxial quantum Wells

4- Microcavities , exciton lasing, polariton lasing

5- Conclusion and a few prospective ideas

- 1- Cristallography, optical properties, basic concepts

Anisotropic optical properties

Identification Tables

Table of OPTICAL PROPERTIES

The optical properties of gem materials

Single refracting or isotropic	Amorphous substances and cubic crystals		One index of refraction, n
Doubly refracting or anisotropic	Hexagonal, Trigonal, Tetragonal	Uniaxial	Two indices of refraction, ω and ϵ; positive, ω less than ϵ; negative, ϵ less than ω
	Rhombic, Monoclinic, Triclinic	Biaxial	Three indices of refraction, α, β and γ; positive, $\alpha\beta$—γ; negative, α—$\beta\gamma$*

*When the intermediate index of refraction β is nearer to α, the optic sign is positive; when nearer to γ, the optic sign is negative.

« Gems: Their sources, Descriptions and identification », edited by Michael O'Donoghue, ELSEVIER 6th edition 2006

C_{6v} known from the shape of wurtzite crystals

CRYSTAL SHAPES FOR HEXAGONAL HOLOHEDRAL HEMIMORPHIC CLASS
Walker, Crystallography, Mc Graw Hill, (1914)

The ZnS class may be easily derived from the holohedral class by dropping the chief plane of symmetry. This means the simultaneous disapearance of the centre and of the six diad axes. Although the hexad axis remains, the forms which meet one end of this axis do not necessarily intersect the opposite end in a similar fashion. The symmetry of this class is therefore one hemimorphic hexad axis, three secondary planes of symmetry and three intermediate planes. On crystals of this class the three prisms characteristic of holohedrism occur but may be distinguished from the corresponding holohedral forms by means of etching figures. The other four forms, viz., basal pinacoid, dihexagonal pyramid and the pyramidss of the first and second orders are each divided into four forms designated respectively upper and lower with the following symbols:

1. Pyramid of the first order, upper (h 0 . ℓ)
2. Pyramid of the first order, lower (h 0 -h -ℓ)
3. Pyramid of the second order order, upper (k k . ℓ)
4. Pyramids of the second order order, lower (k k . -ℓ)
5. Dihexagonal pyramids, upper (k i . ℓ)
6. Dihexagonal pyramids, upper (k i . -ℓ)
7. Basal pinacoid, upper (0 0 0 1)
8. Basal pinacoid, lower (0 0 0 -1)

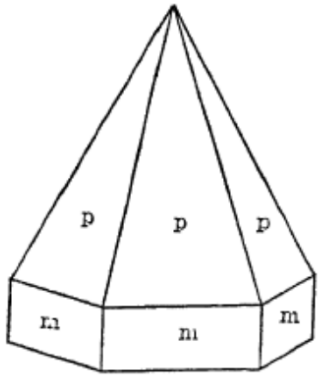

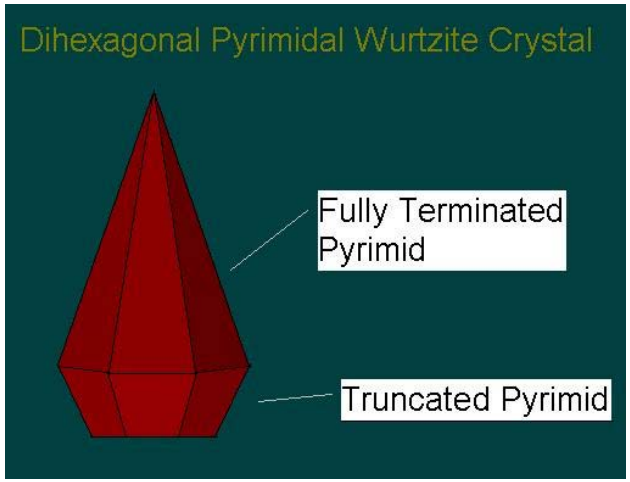

☛$P6_3mc$ or C^3_{6V} identified by W.L.Bragg in 1920

11.2. Highlights of Structure Determination

Some highlights in determining the important structure types occurring in minerals shall be mentioned now, regardless of whether the determinations were done by physicists, chemists or mineralogists.

1913: The first structure determinations (W. H. and W. L. Bragg) were done on the minerals zincblende, diamond and NaCl. It still appears miraculous to the writer how fortunate and ingenious the Braggs were in chosing these 'easy' substances, considering how many much more complex structures could have been picked.

1914: Copper (W. L. Bragg); CaF_2 (W. L. Bragg); FeS_2 (W. L. Bragg).

1915: Spinel (W. H. Bragg, independently Nishikawa); calcite (W. H. Bragg).

1916: Graphite (Debye and Scherrer; independently Hull in 1917); rutile and anatase (Vegard).

1919: $Mg(OH)_2 = CdJ_2$-type (Aminoff).

1920: Wurtzite (W. L. Bragg).

1923: NiAs (Aminoff).

1924: The first silicate, garnet (Menzer).

1925/1926: SiO_2 — structures (W. H. Bragg and Gibbs; Wyckoff; Seljakow, Strebinski and Krasnikow).

1923–1926: V. M. Goldschmidt's famous rules of Crystal Chemistry and the determination of the size of atoms and ions. The main rule may be quoted here in the original formulation (*Geochemische Verteilungsgesetze der Elemente*, VII, pg. 9):

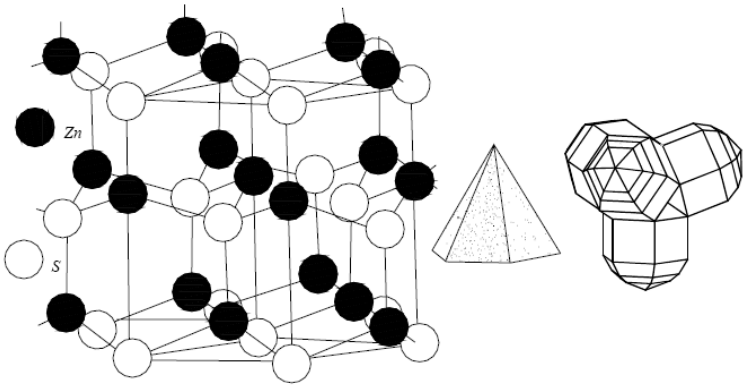

wurtzite structure, crystals and twin

The wurtzitic crystal is an efficient natural dipole

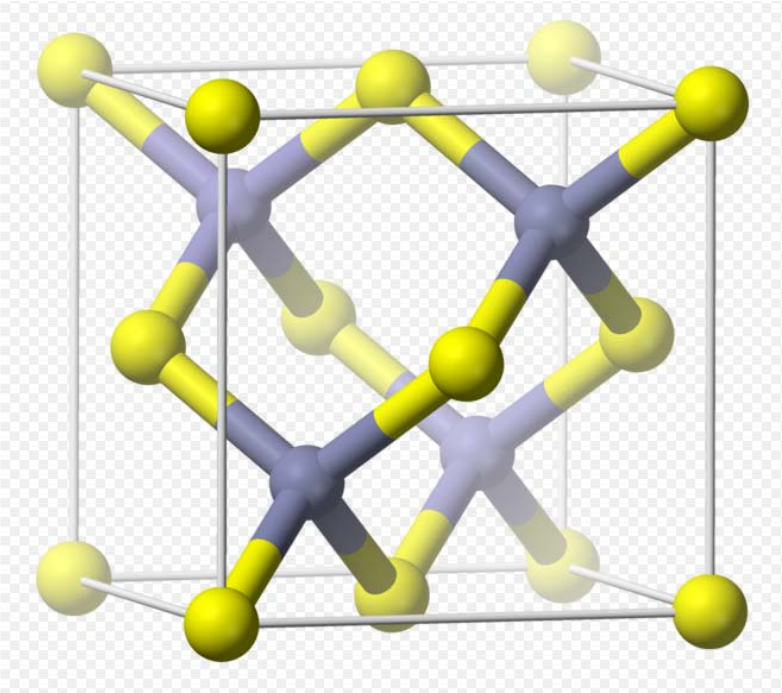

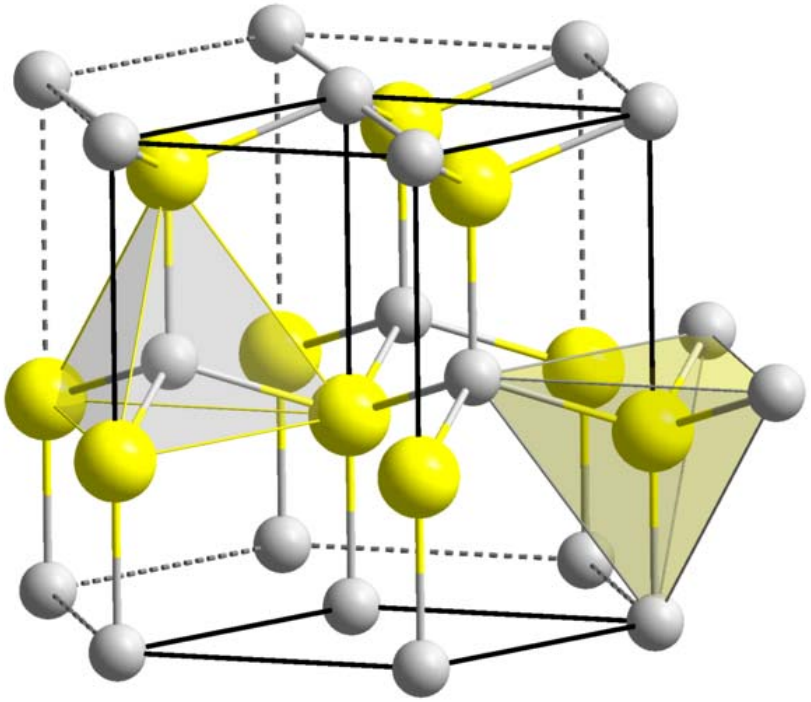

Polar , non polar and semipolar reticular planes

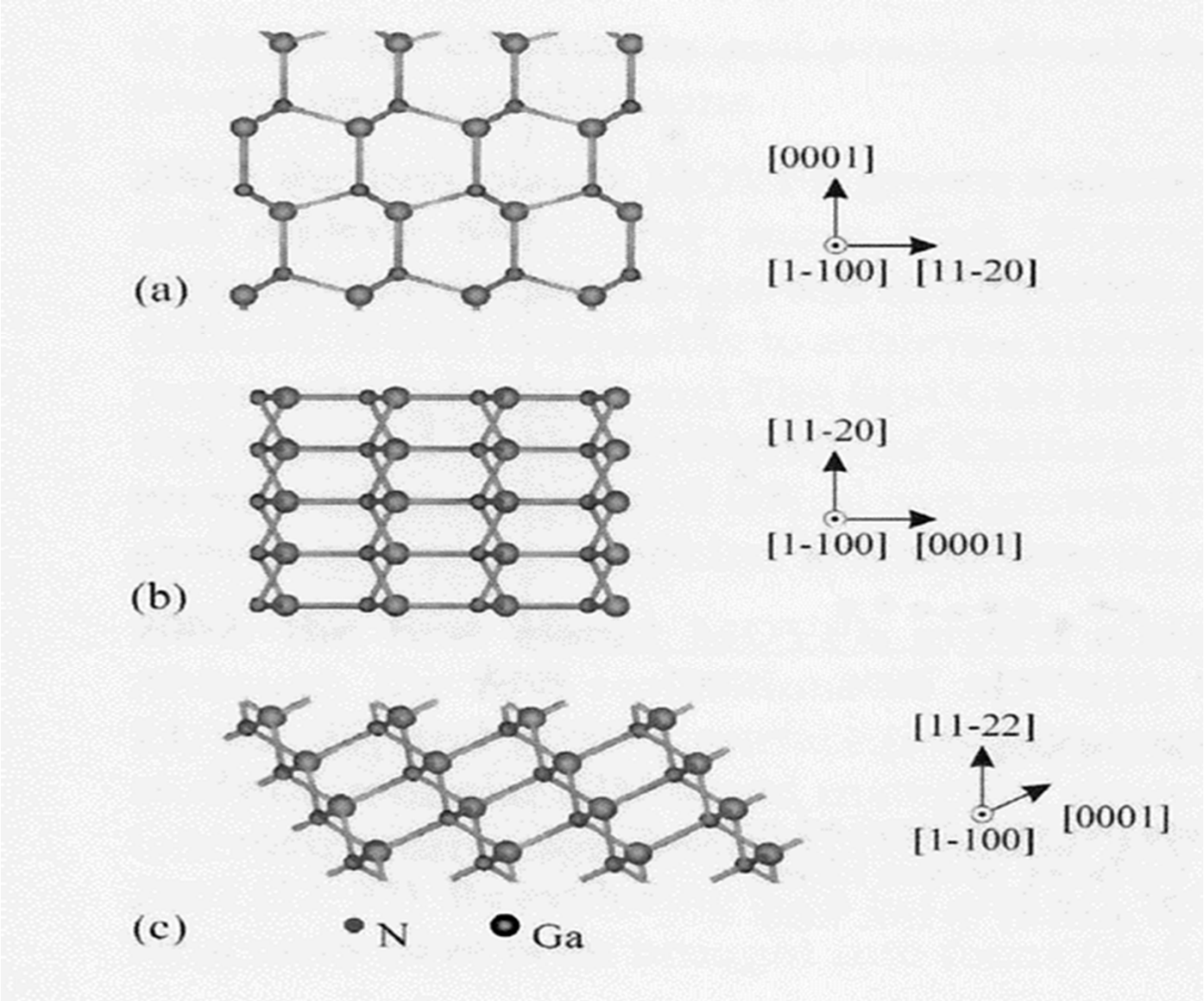

Possible discontinuity of the polarization at heterointerfaces

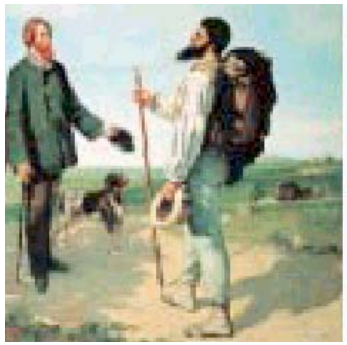

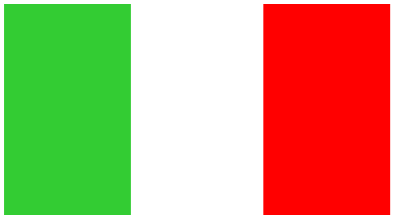

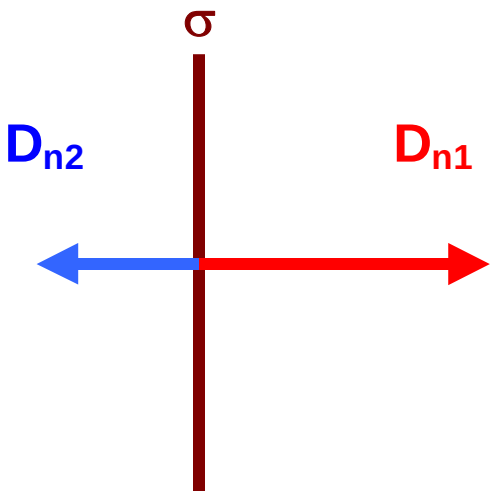

$D_{n1} - D_{n2} = \sigma$

F. Bernardini, V. Fiorentini and D. Vanderbilt, Phys. Rev. B **56**, R10024 (1997)

F. Bernardini and V. Fiorentini, Phys. Rev. B **57**, R9427 (1998)

Heterostructure with strong orientation-dependent optical properties

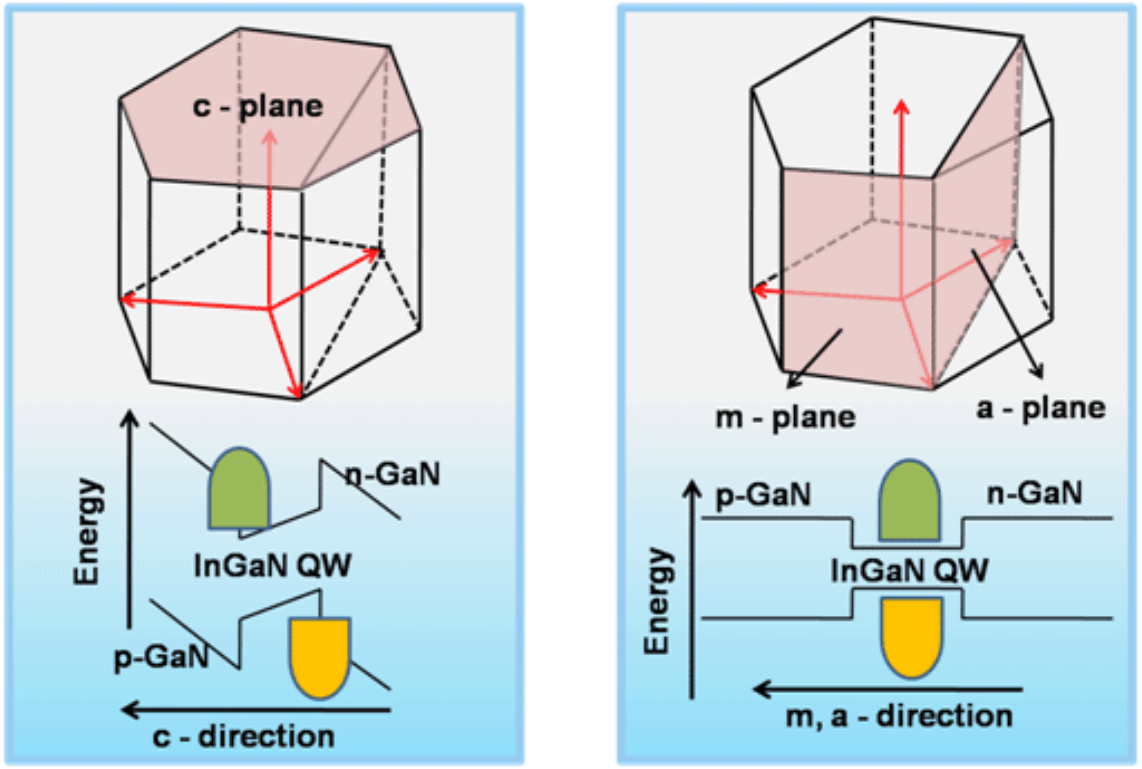

Non – polar direction GaN thin film growth ➔ higher quantum efficiency

Record optical properties

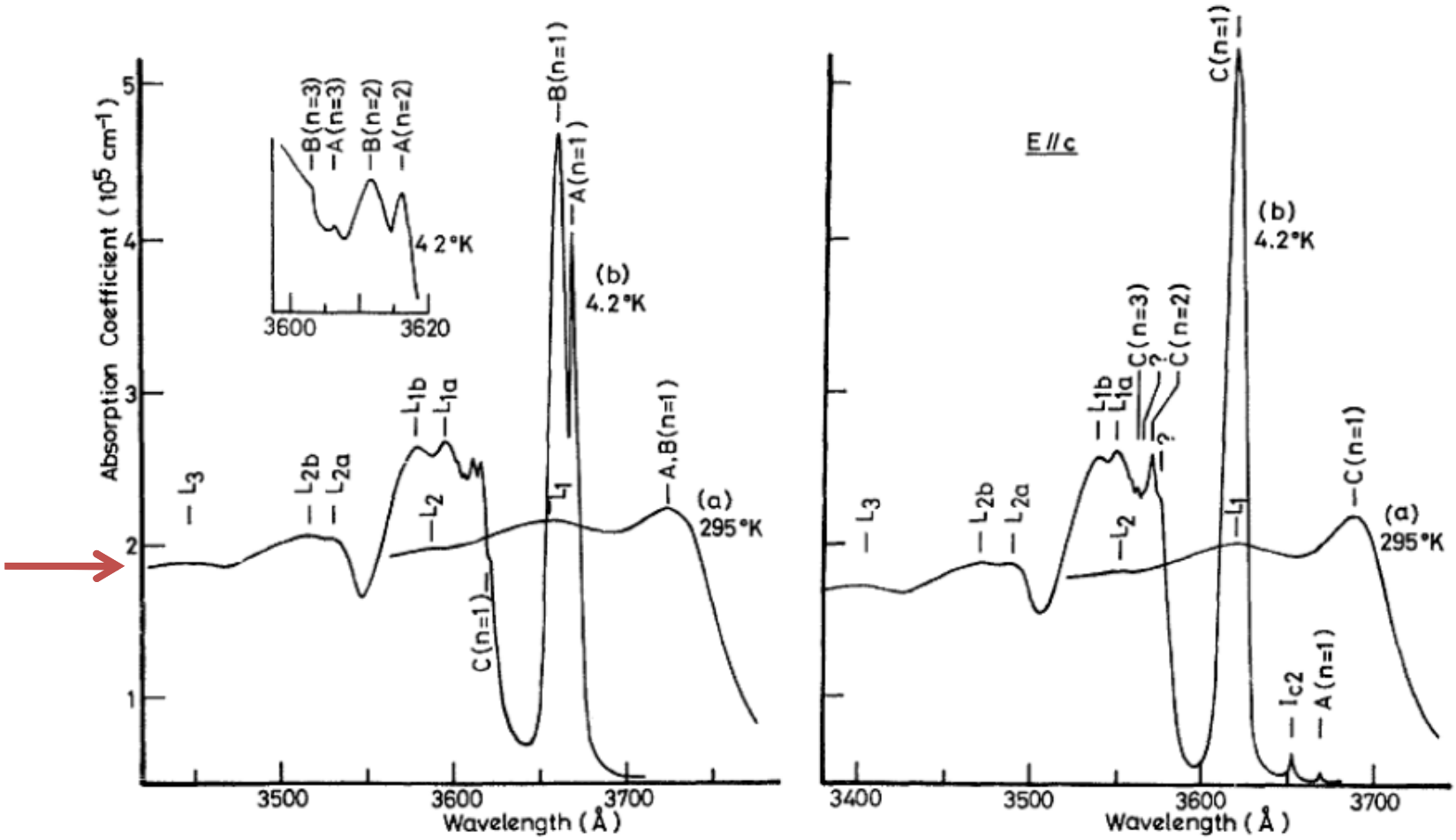

WY. Liang and AD. Yoffe Physical Review Letters, **20 ,** 59, (1968)

Valence band structure 1

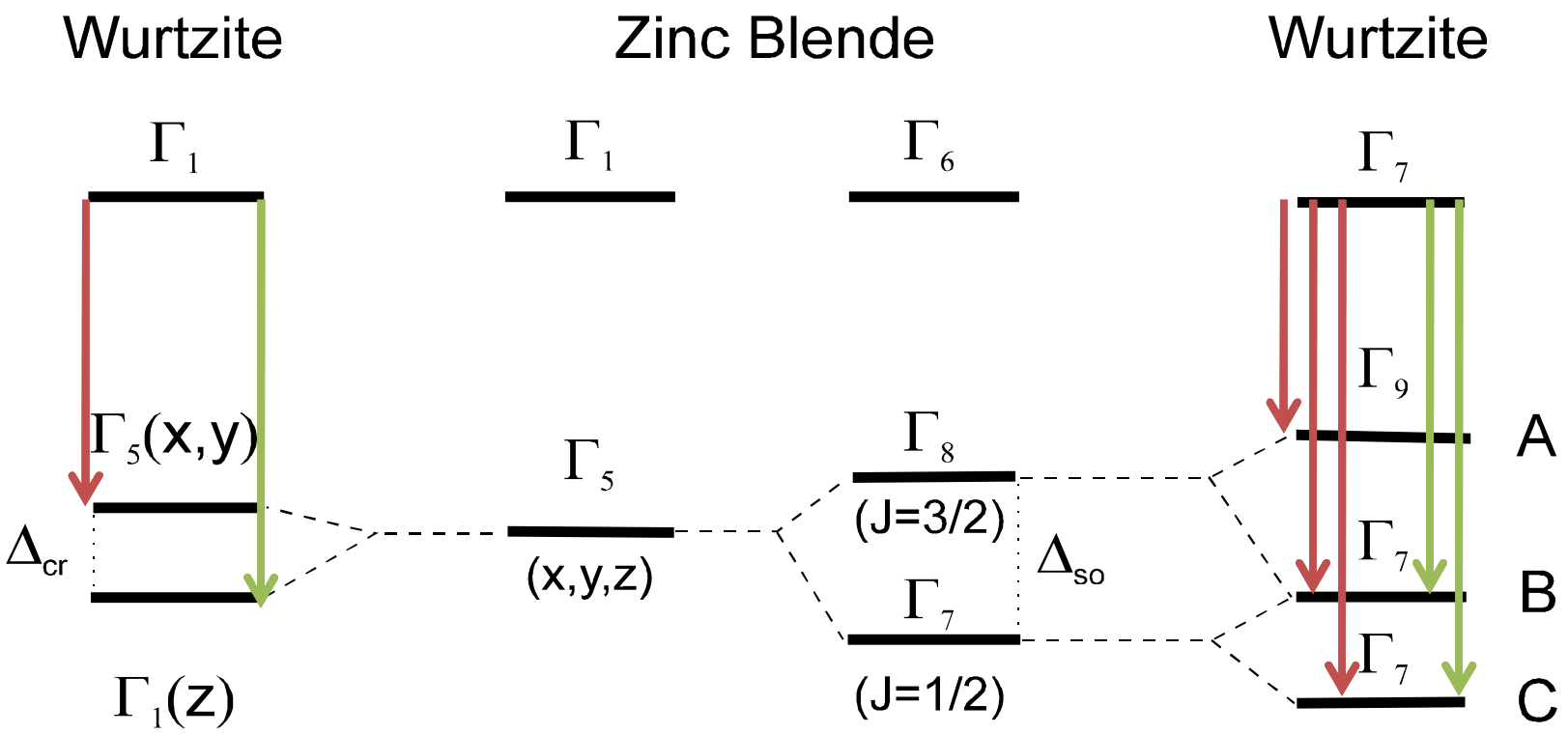

Simple Group

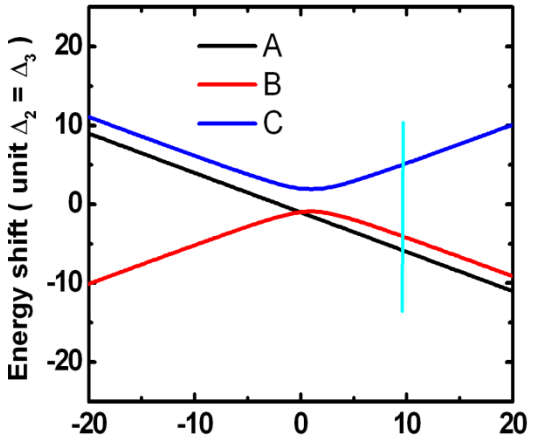

Valence band structure 2

Δ_{cr} ~ 30 meV

Δ_{cr} >> Δ_{so}

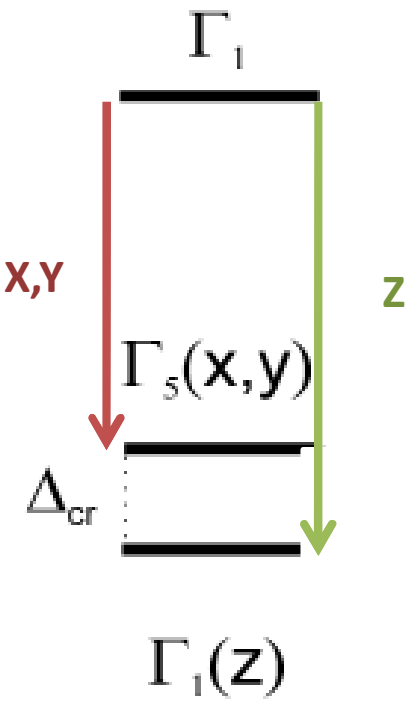

Reynolds et al. PRB **60**, 2340, (1999)

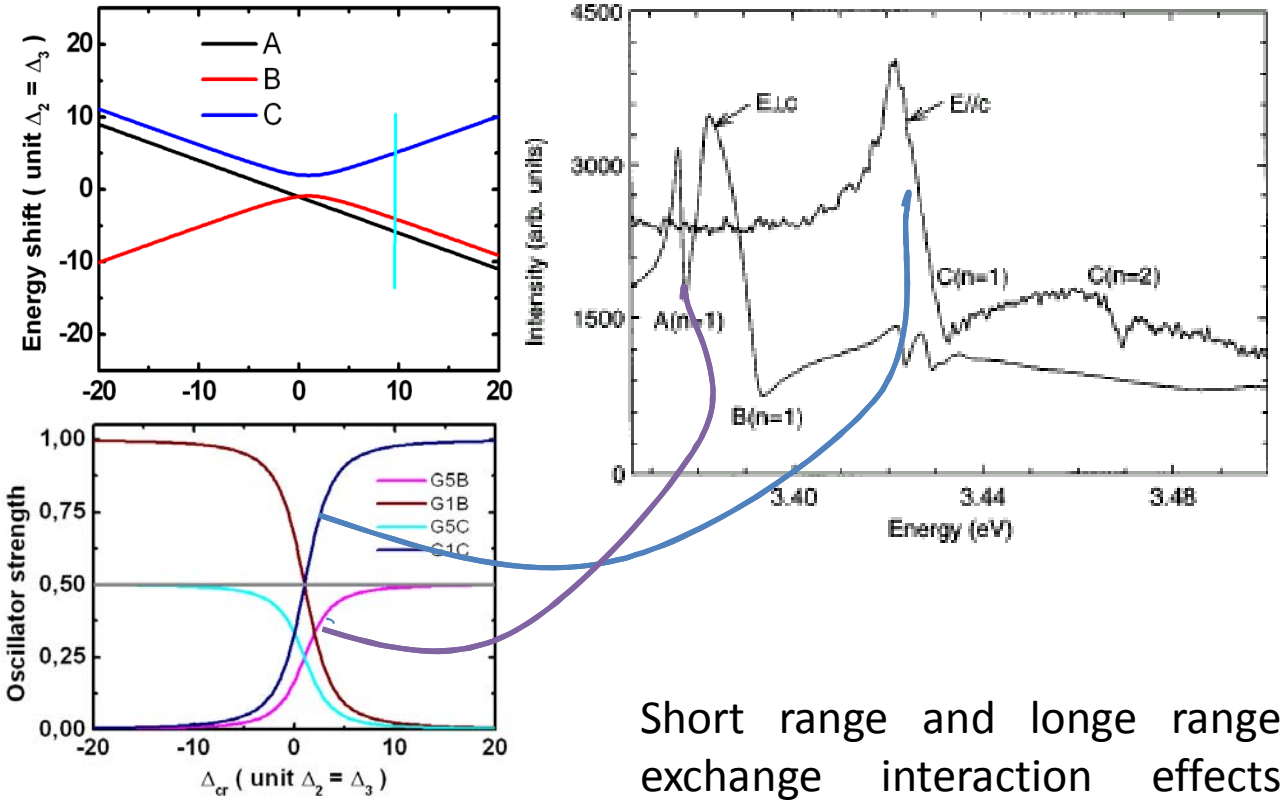

Short range and longe range exchange interaction effects should be included for giving a more appropriate vision of the actual situation

2- Optical properties of heteroepitaxial polar ZnO-ZnMgO Quantum Wells

Work in collaboration with CRHEA (crystal grower C.Morhain)

Quantum wells grown along polar orientations

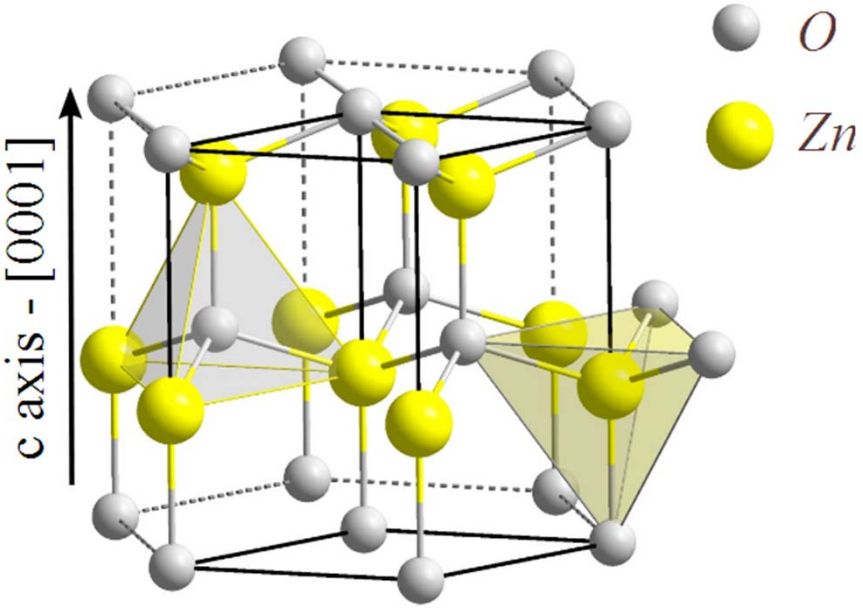

Wurtzite crystal structure

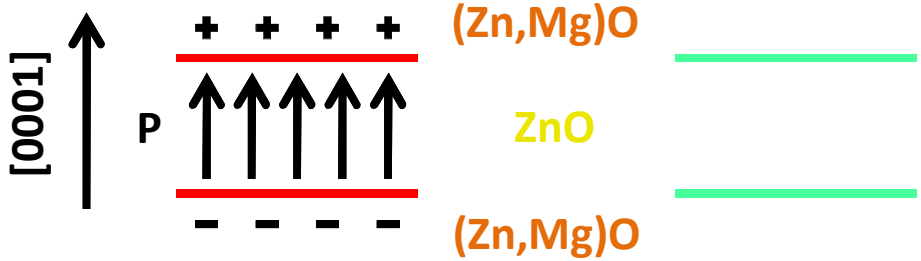

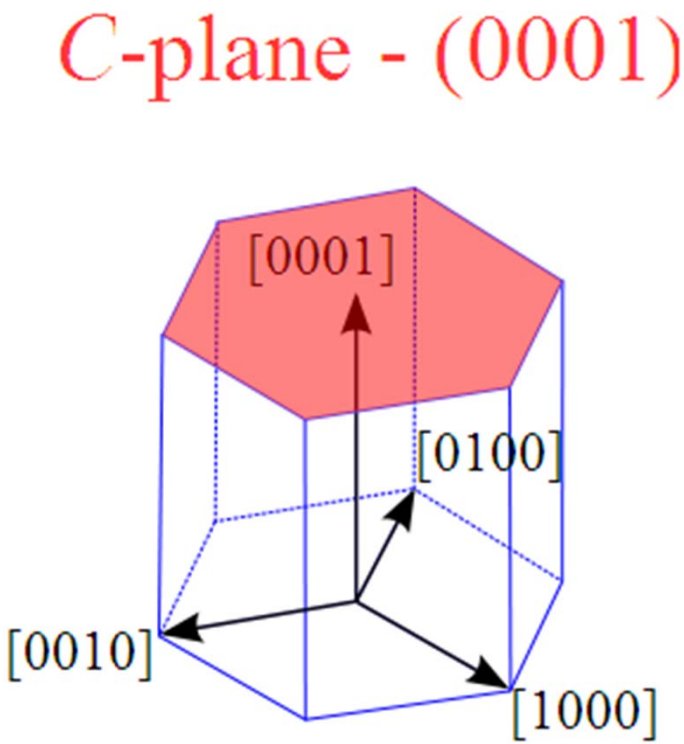

In-plane isotropy of the optical response

Our ZnO- $Zn_{1-x}Mg_xO$ QW Samples

- C. Morhain, CRHEA
- MBE growth
- Special care for a 2D growth
- Large variety of well widths (1.6 - 9.5 nm)

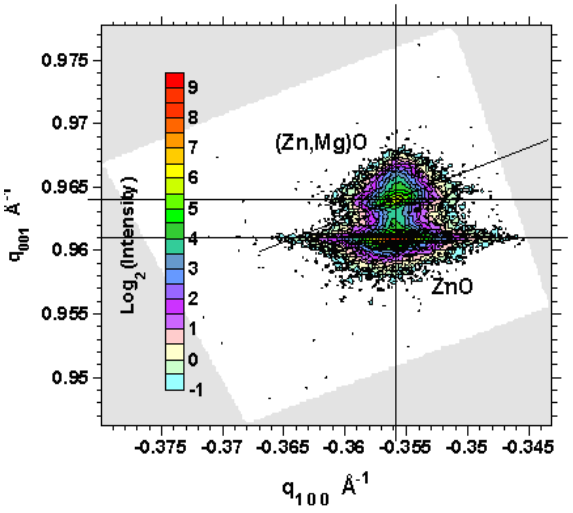

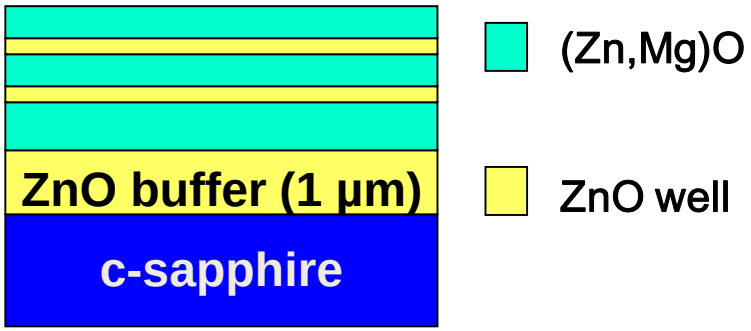

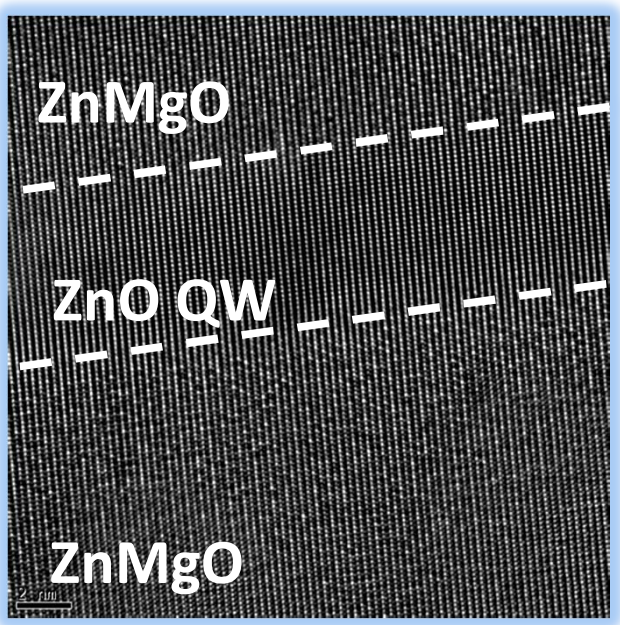

C. Morhain et al., Superlat. and Micr. 38, 455 (2005)

Quantum Confined Stark Effect

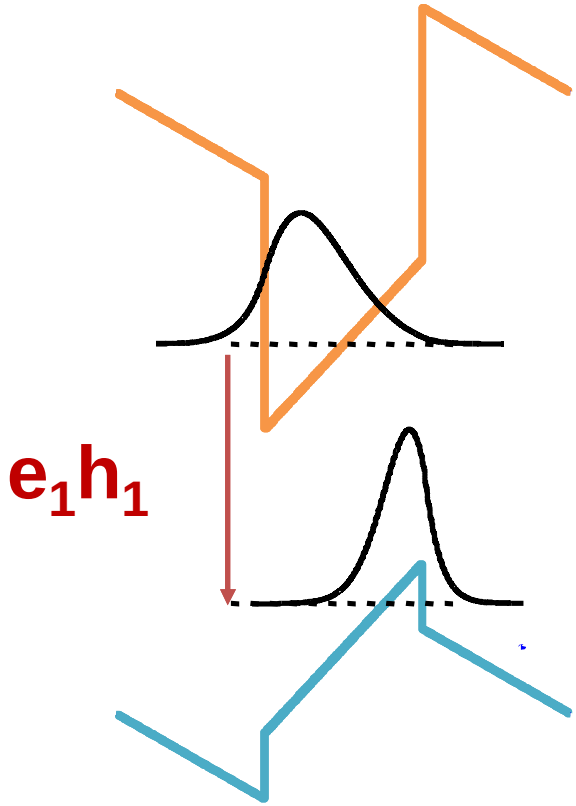

➢**Wide QWs ⇒ The Quantum Confined Stark Effect *can* dominate**

- Transition energy decreases with increasing well width (QCSE) (~ linear in L_W)
- The oscillator strength of e_1h_1 decreases with increasing well width (~exponential in L_W)

⇒ The PL decay time increases and it can reach ms

➢**Narrow QWs ⇒ Quantum Confinement dominates**

- much more moderate behaviors of energy and decay times with well width than in previous case

Getting the transition energy by using photoluminescence

- Screening of the internal electric field
- Determination of the fondamental energy is difficult

Blue shift in emission energy from 6.5nm QW with increasing excitation energy

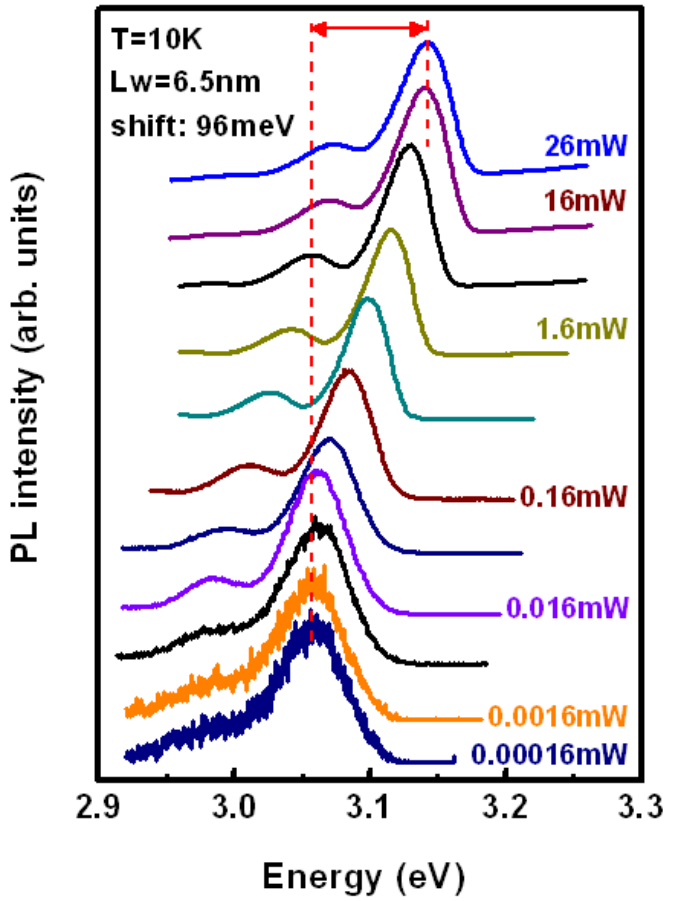

Screening of the electric field TR PL

$GaN/Al_{0.15}Ga_{0.85}N$ QW. L = 7.8 nm

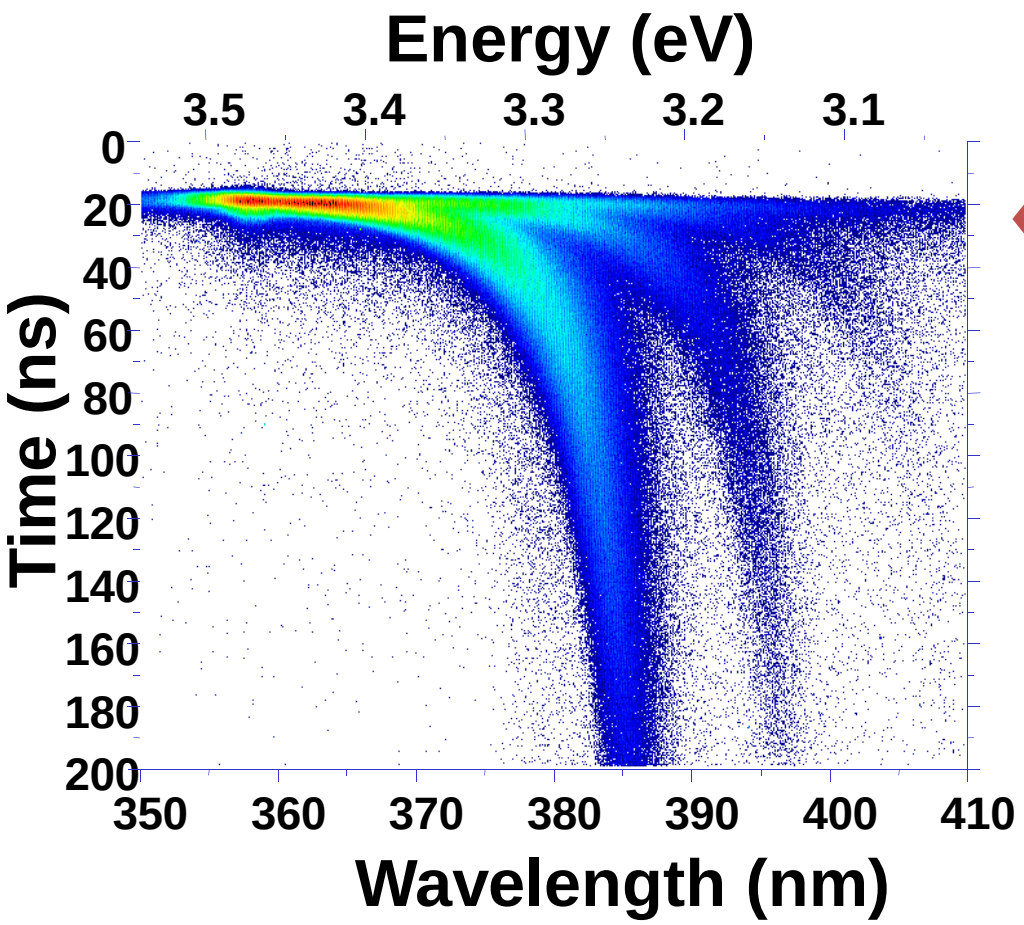

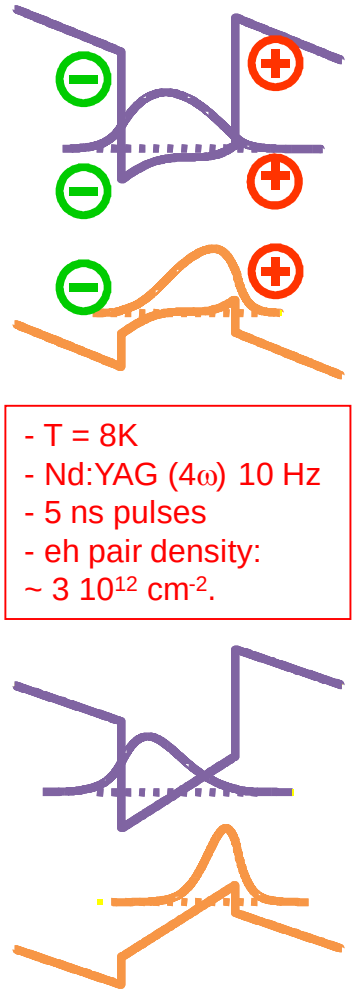

- T = 8K
- Nd:YAG (4ω) 10 Hz
- 5 ns pulses
- eh pair density:
~ 3 10^{12} cm^{-2}.

Phys. Rev. B 69, 035307 (2004)

Time-integrated PL and TRPL

- Extraction of the un-screened regime
- Constant PL energy and exponential decay

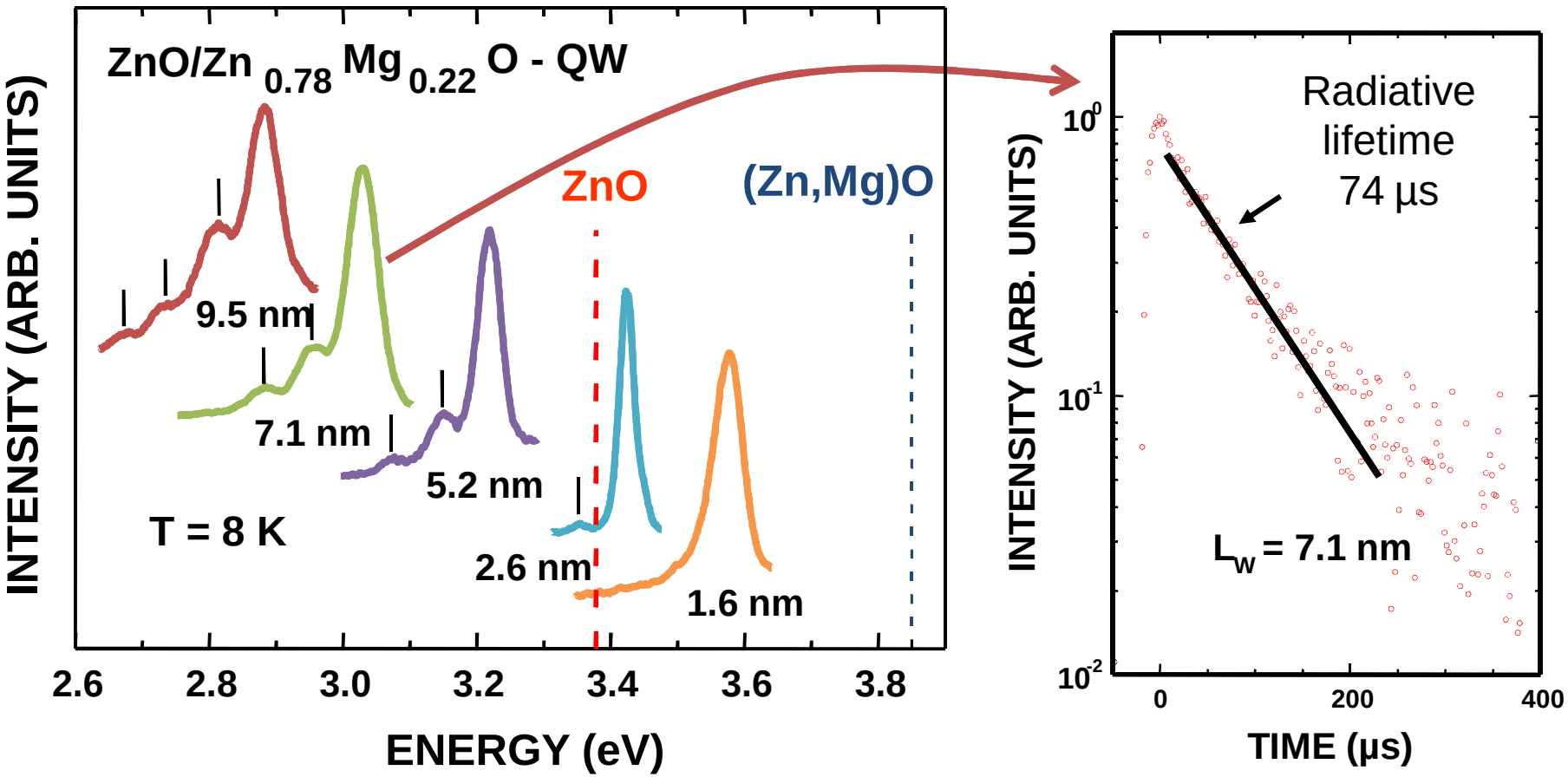

Determination of the piezo electric field from carefully done PL

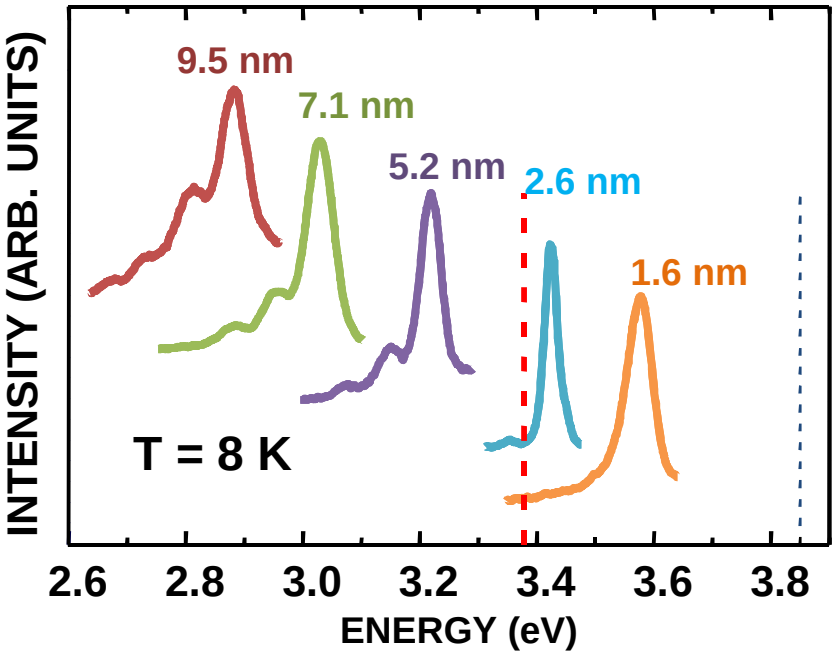

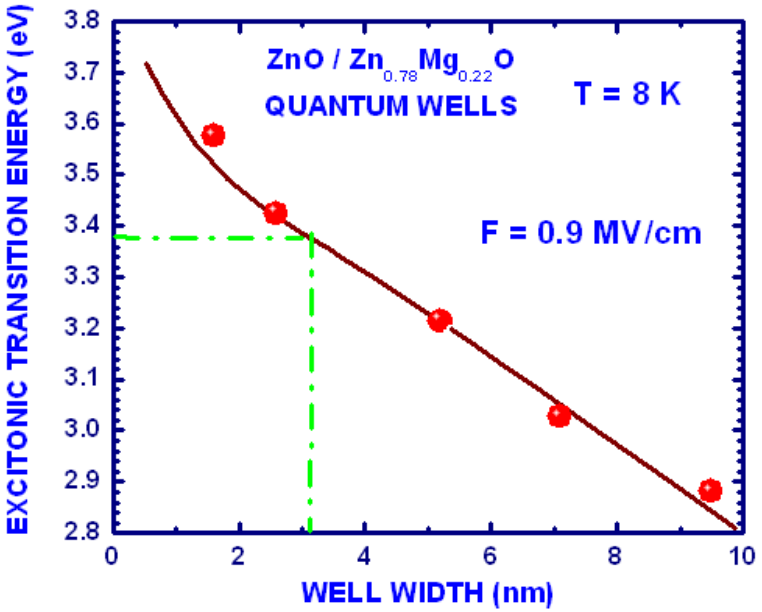

Exciton binding energy in ZnO-based QWs

$$\Phi_{1s}(r,z_e,z_h)=f_e(z_e)\cdot f_h(z_h)\cdot N\cdot\exp(-r/\lambda)$$

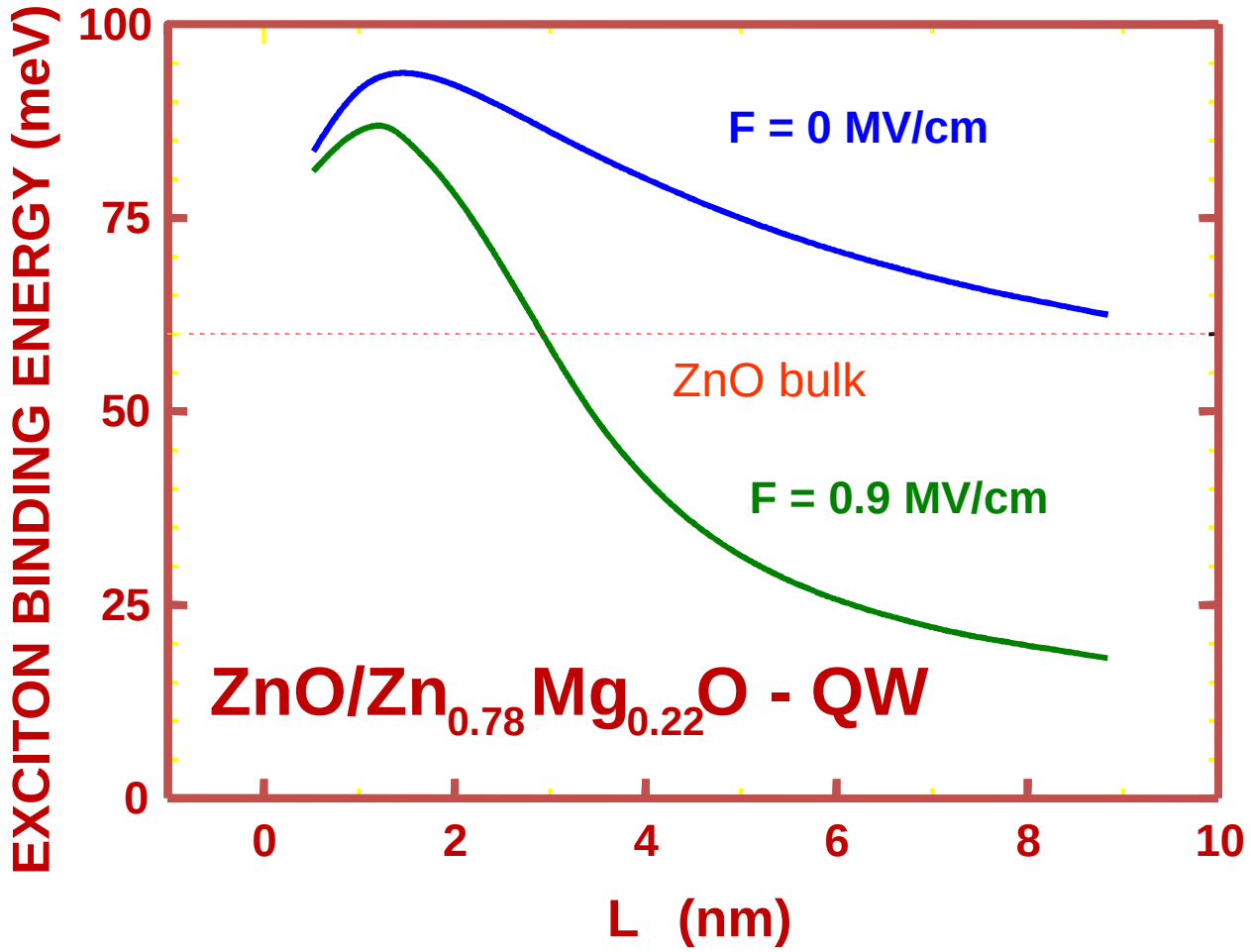

Quantum Confined Stark Effect

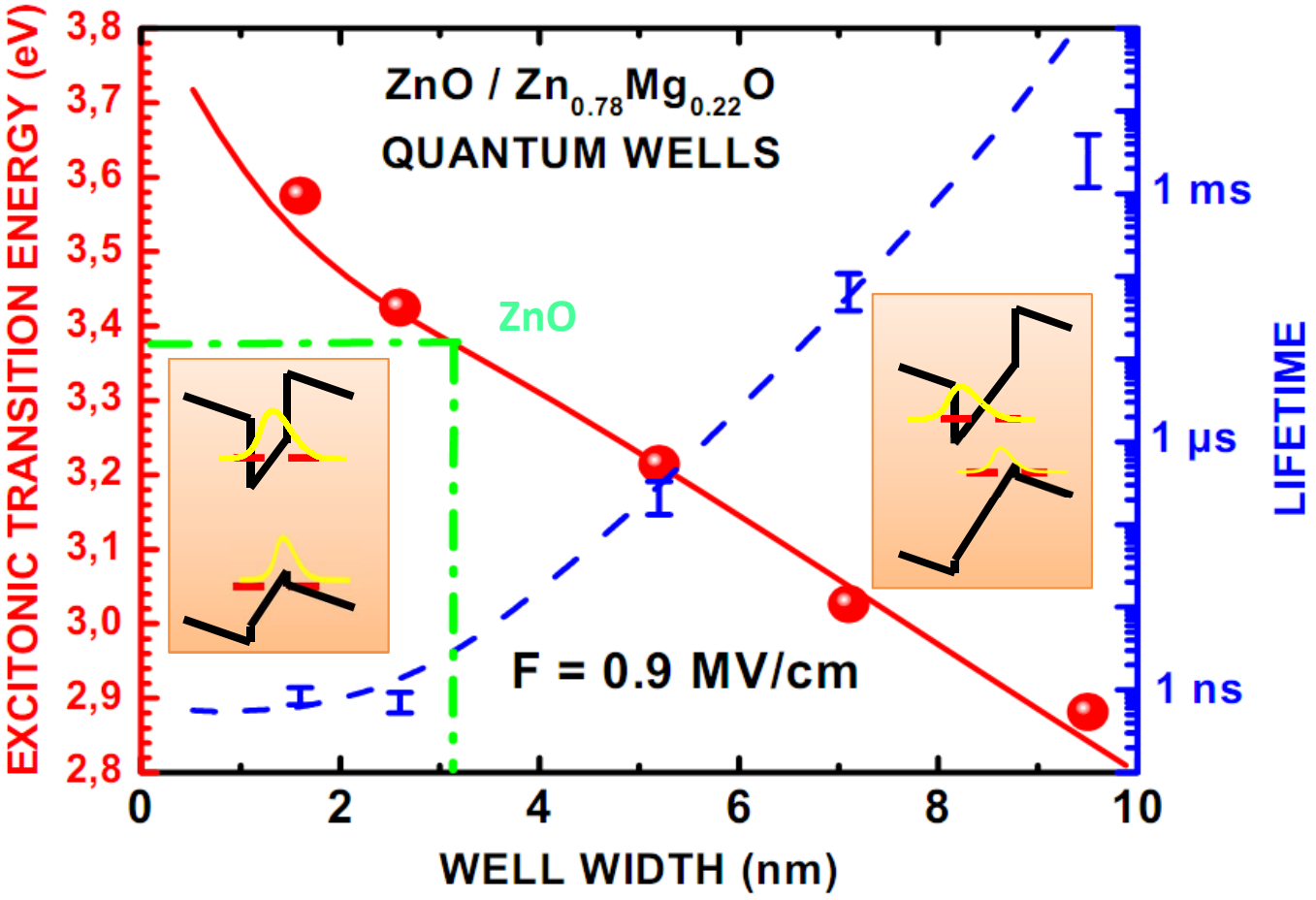

C. Morhain, T. Bretagnon et al, Phys. Rev. B **72**, 241305 (2005)

Effect of barrier composition

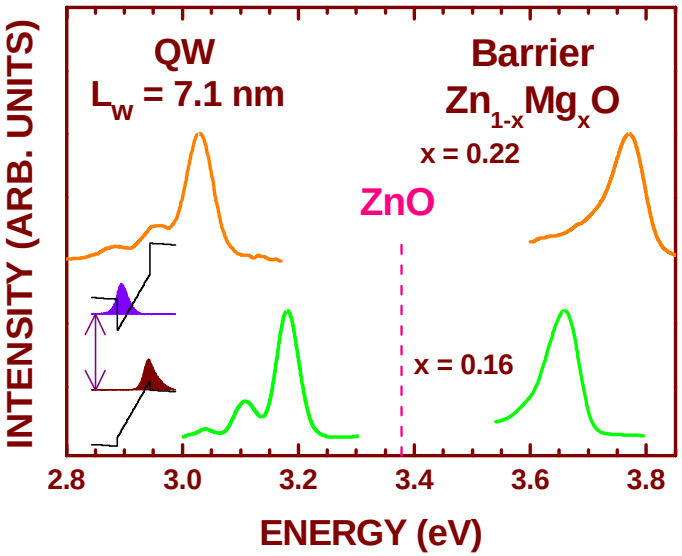

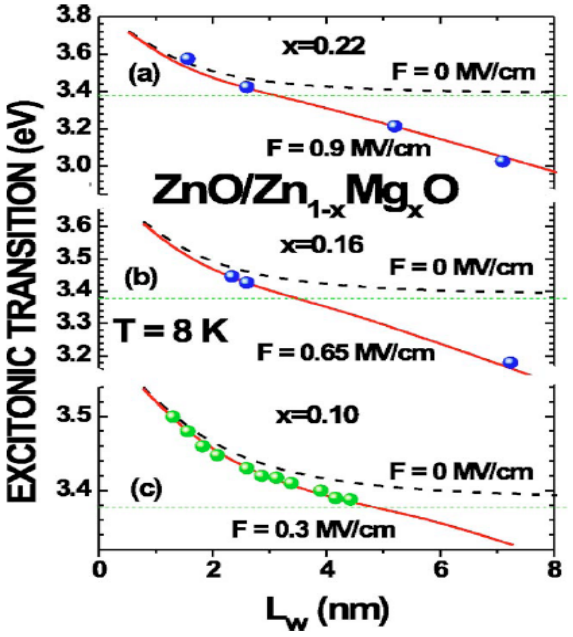

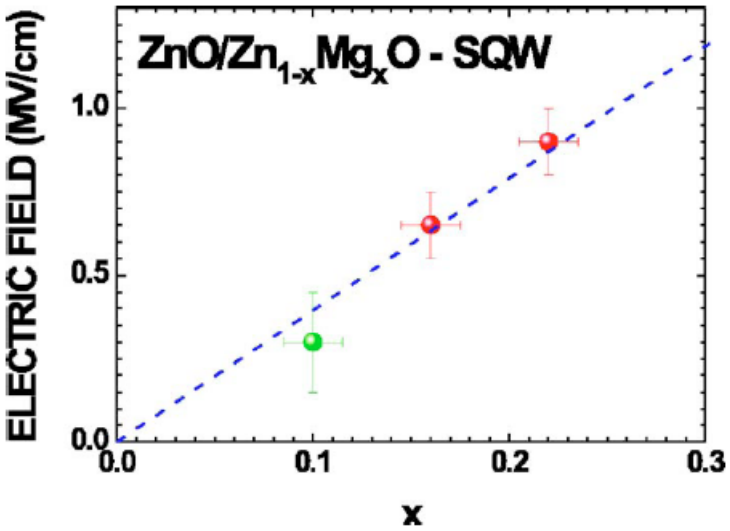

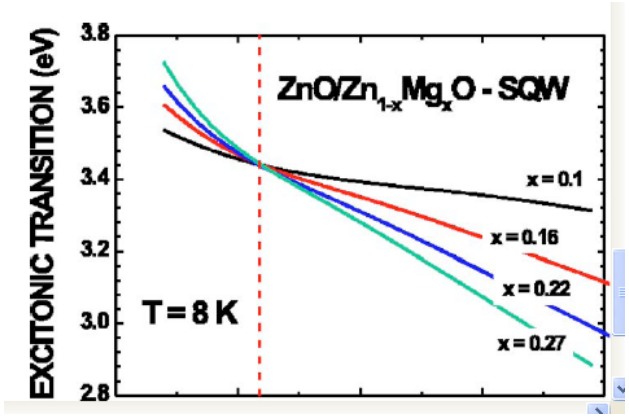

T. Bretagnon et al, Appl. Phys. Lett. ***90****, 201192 (2007)*

Very bad robustness of PL with T

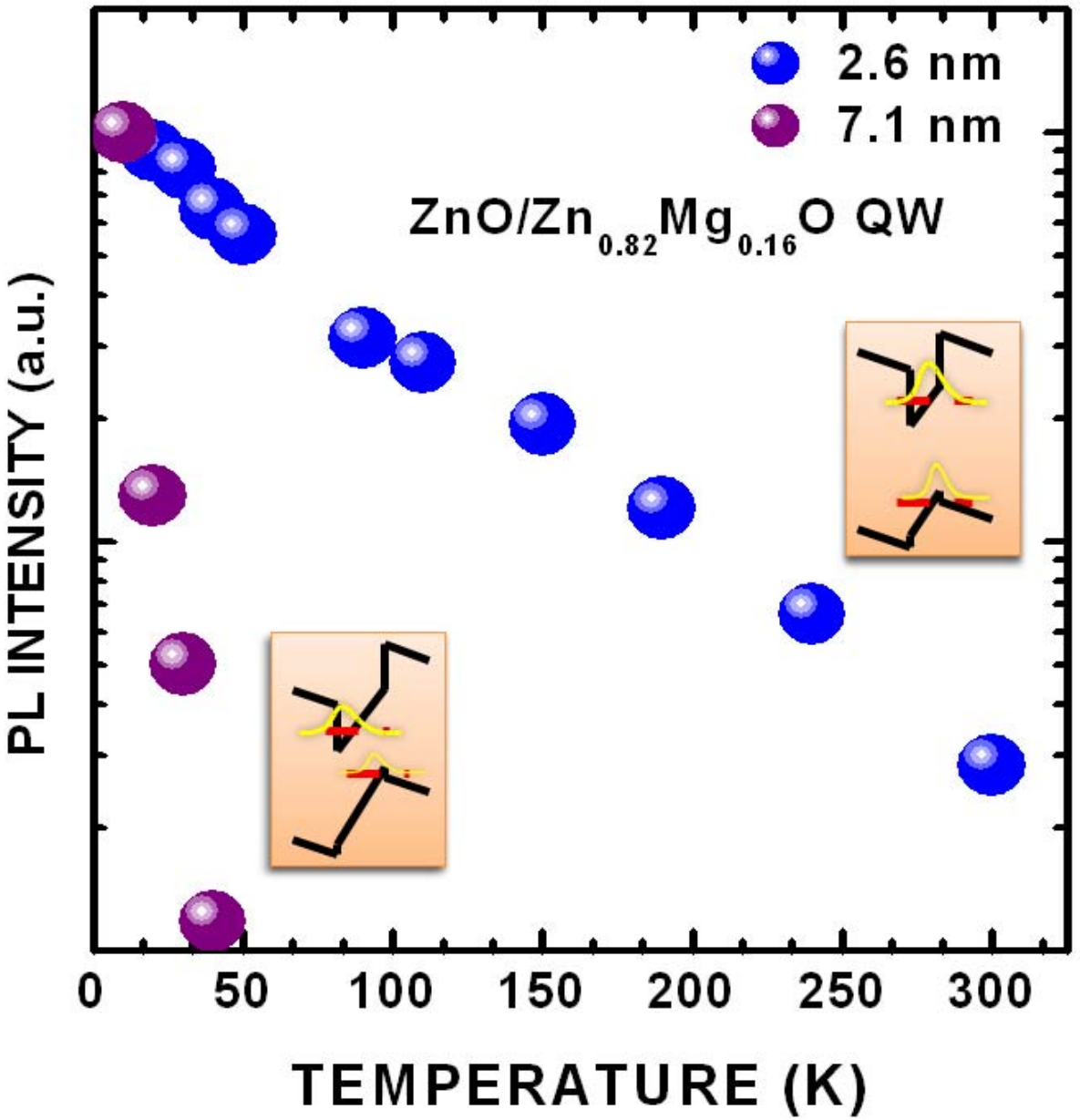

Phonon-assisted exciton formation

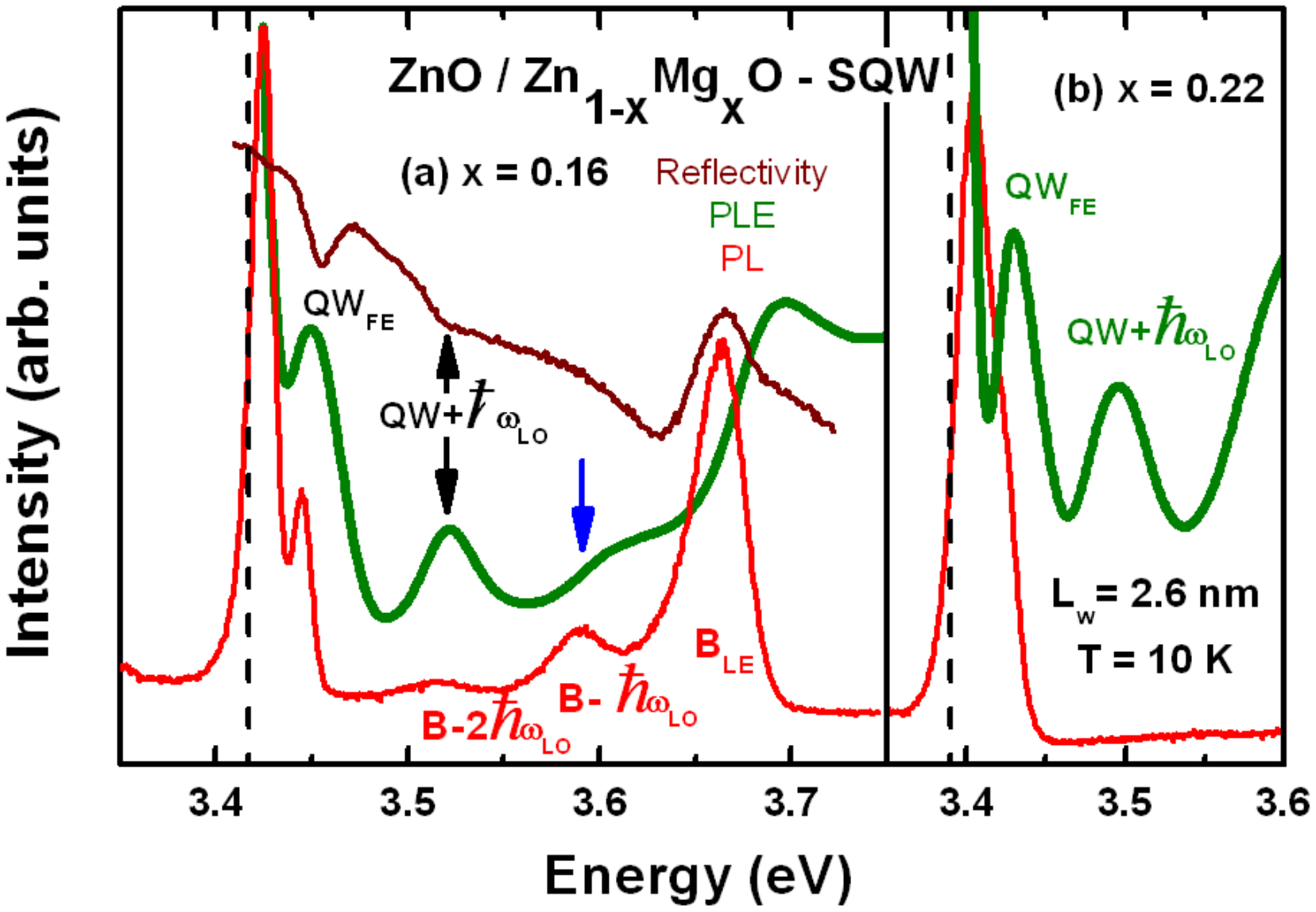

3- Optical properties of M-plane oriented nonpolar homoepitaxial quantum wells

Work in collaboration with CRHEA (crystal grower J.M.Chauveau)

In-plane anisotropic optical properties of M-plane oriented nonpolar homoepitaxial quantum wells

Bulk ZnO substrates now available, notably non-polar M-plane ZnO

MBE growth of non-polar M-plane ZnO/(Zn,Mg)O QW (J.M. Chauveau, CRHEA)

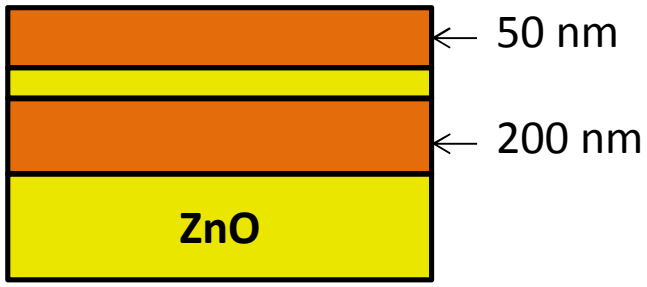

L_w = 1.1 to 6.2 nm
Mg content = 20 %

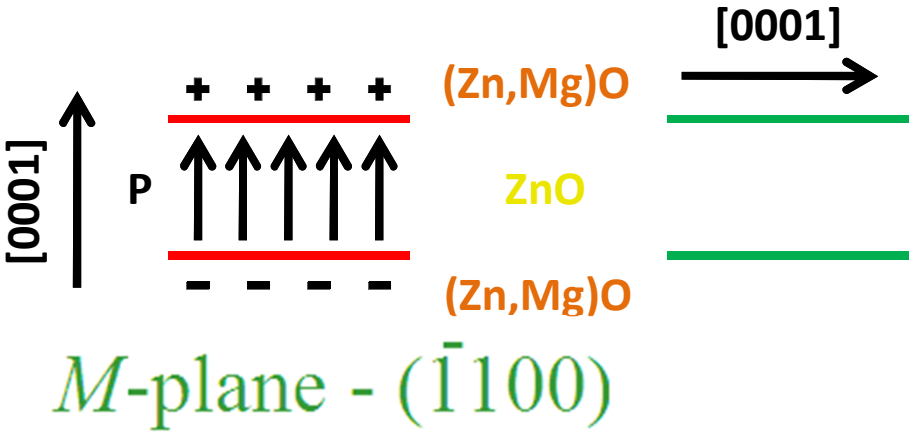

M-plane - ($\bar{1}100$)

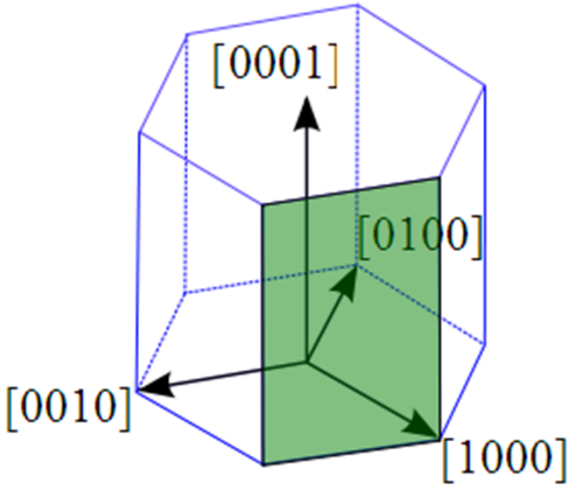

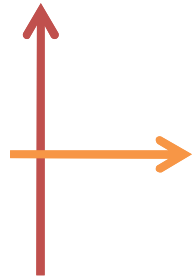

non-polar

Anisotropic optical properties

Unpolarized PL

λ_{exc}= 244nm

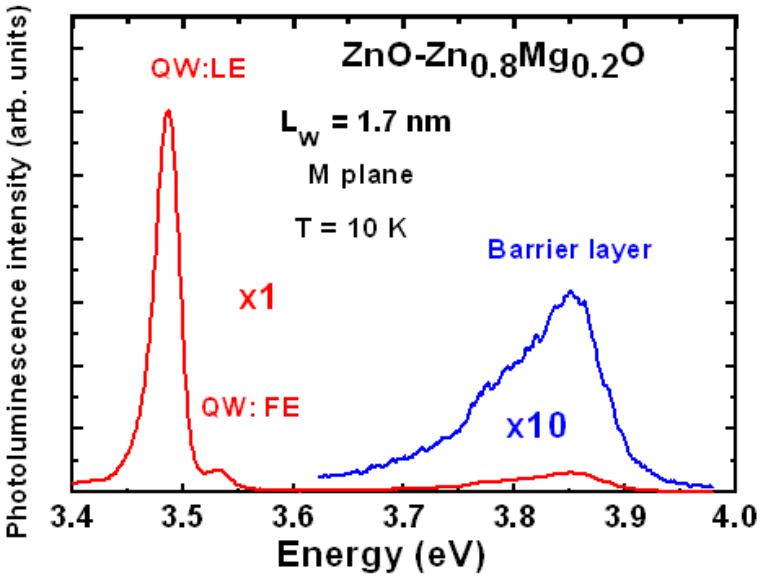

Polarized PL and Reflectance

λ_{exc}= 325nm

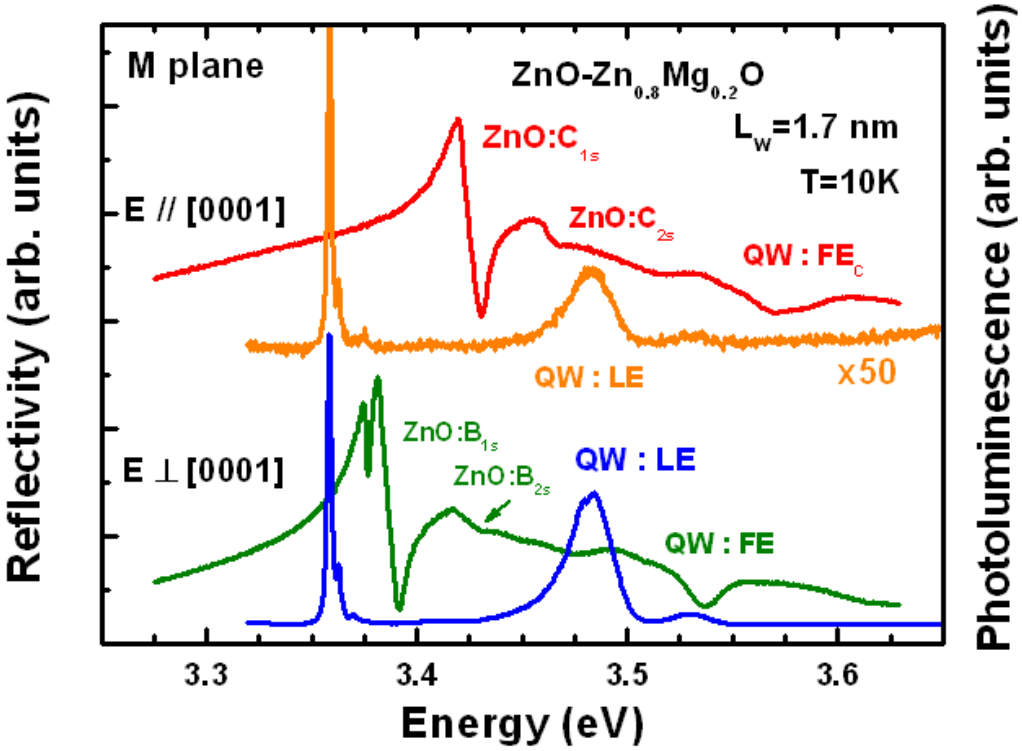

Selection rules and report of observation of excited states

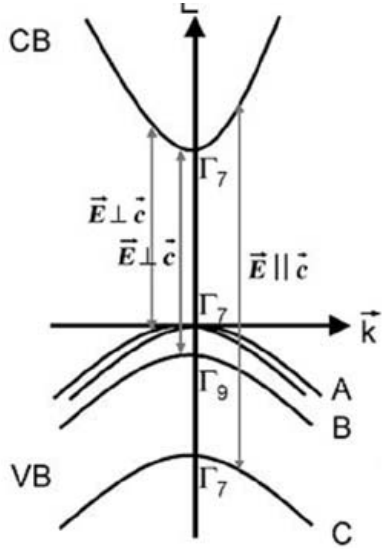

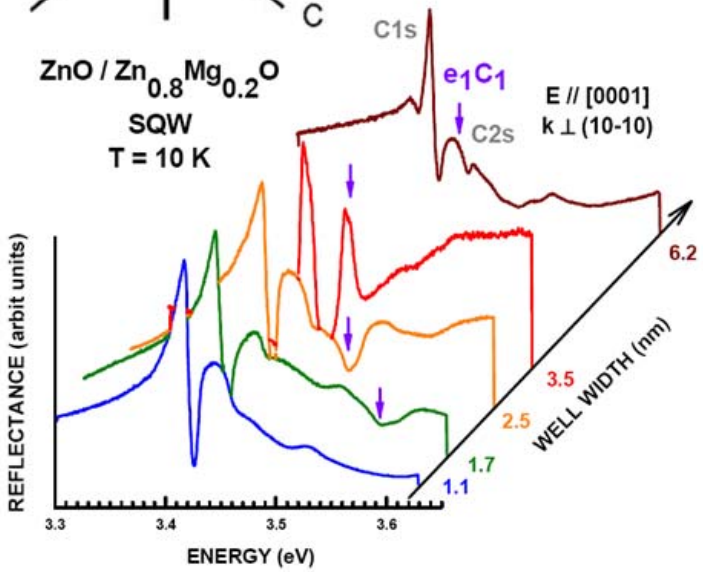

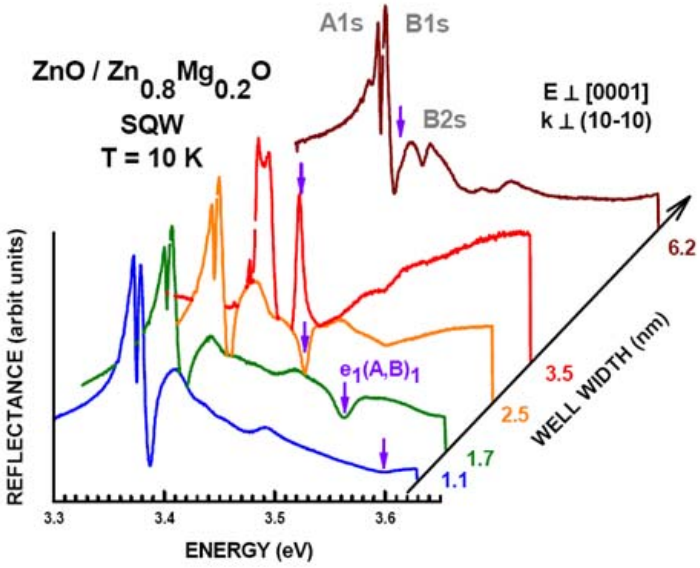

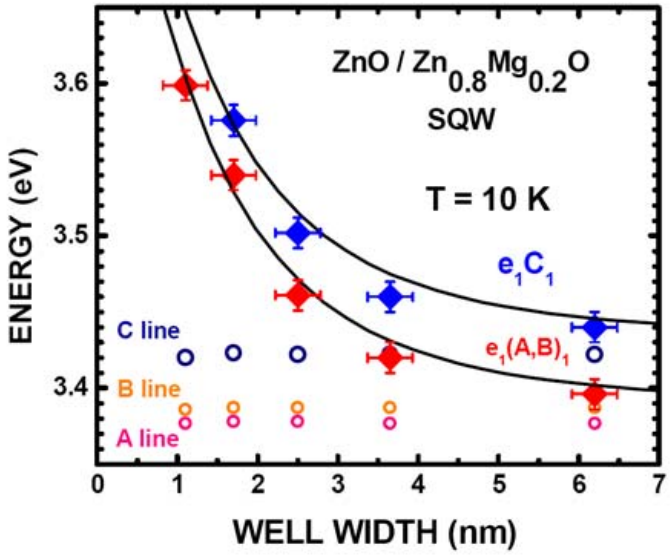

M-Plane QWs: robust PL above RT

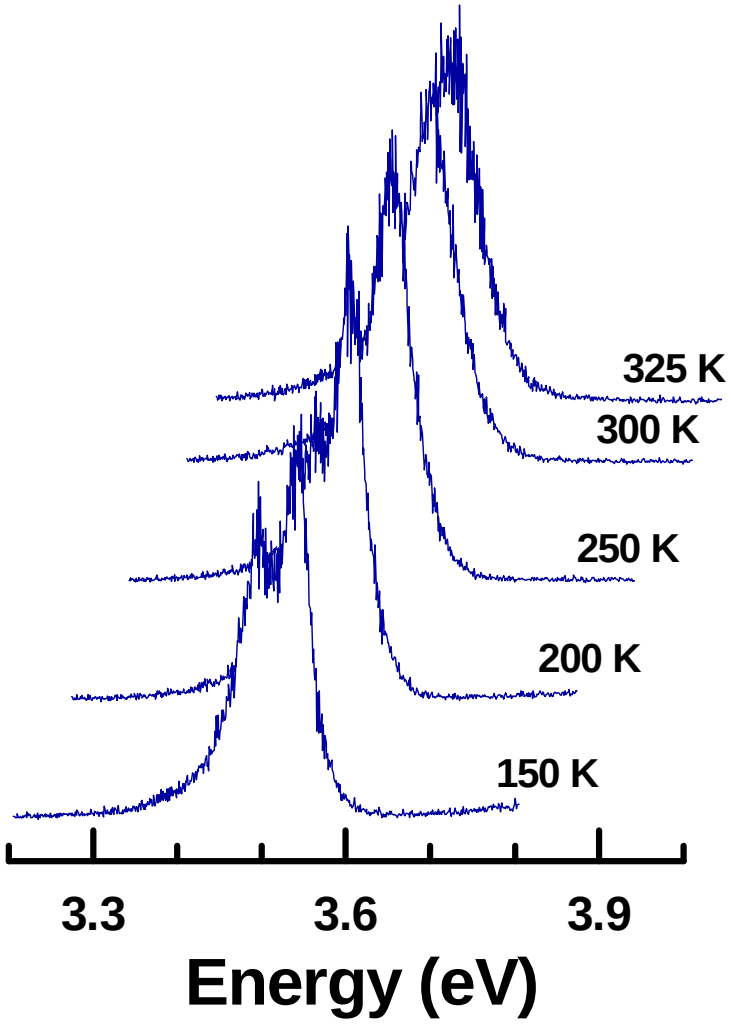

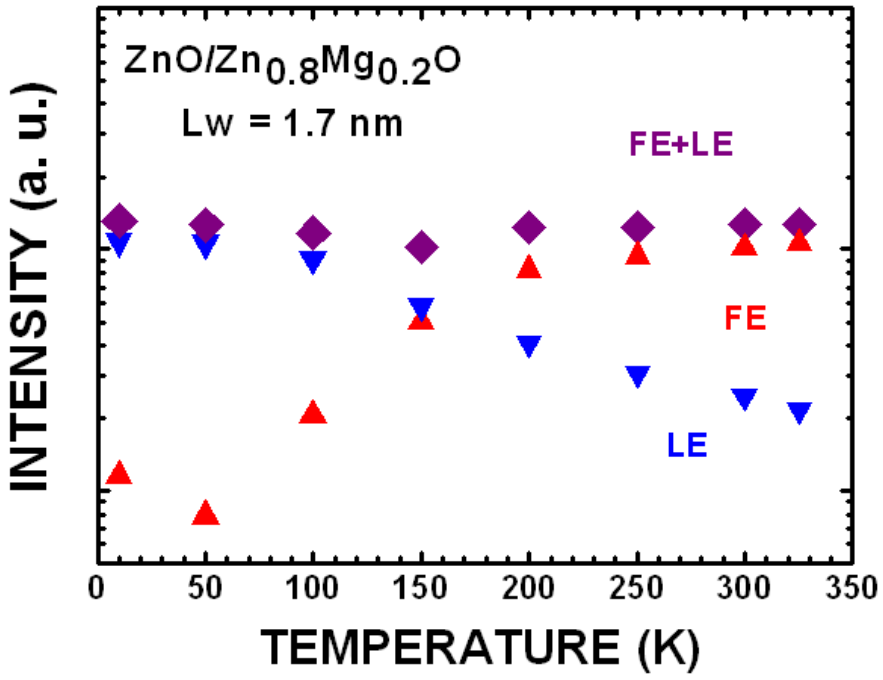

Perfect growth leading to the eradication of non radiative recombination channels

Radiative decay time increases linearly with T: the text book situation

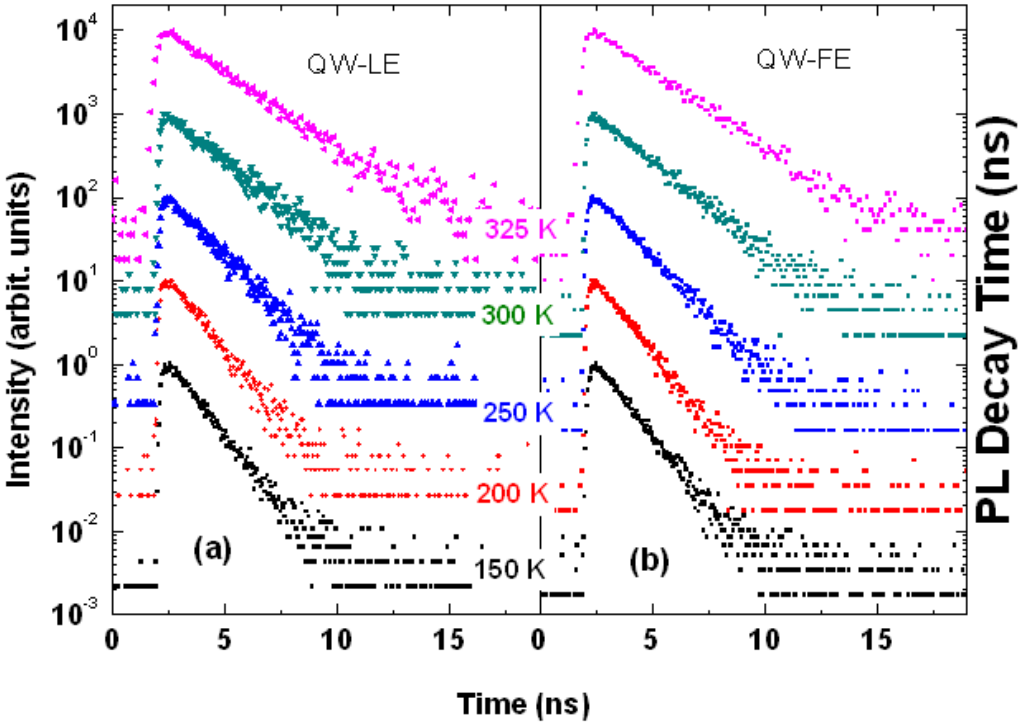

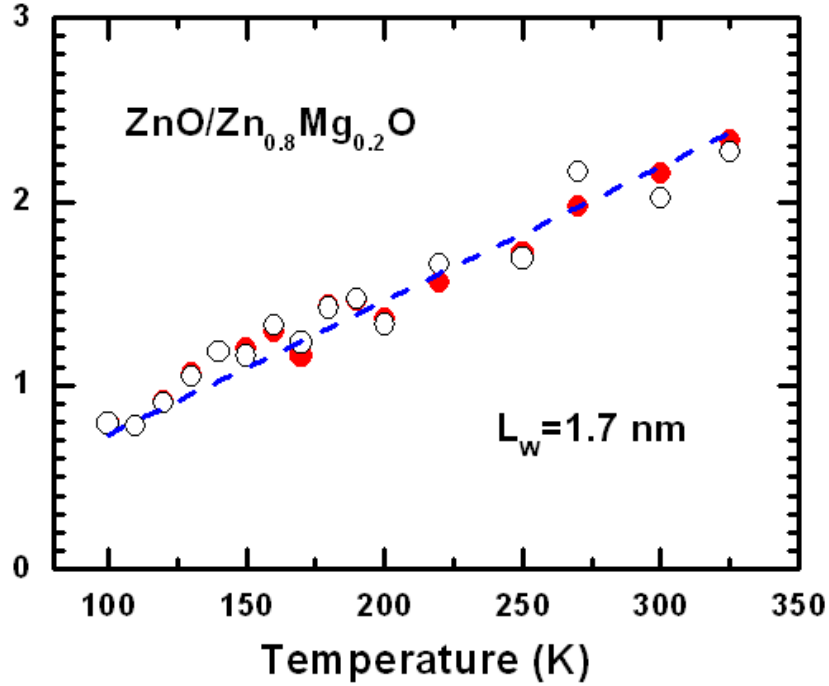

Electronic Structure- PL

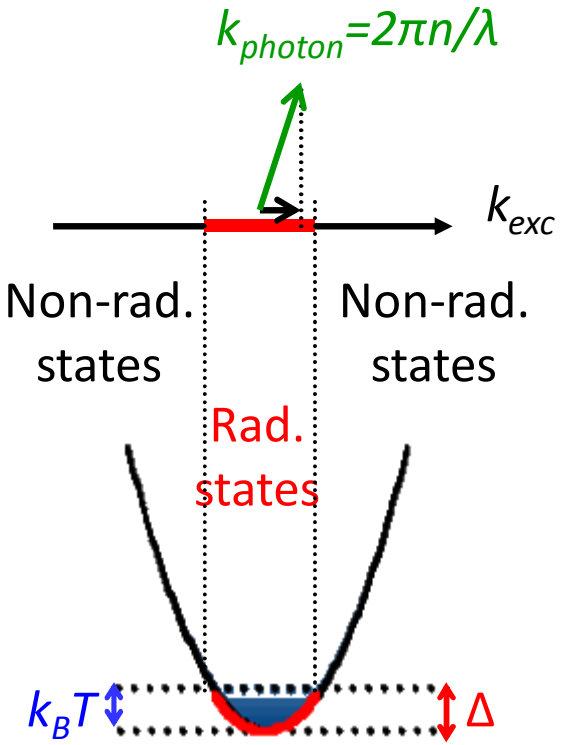

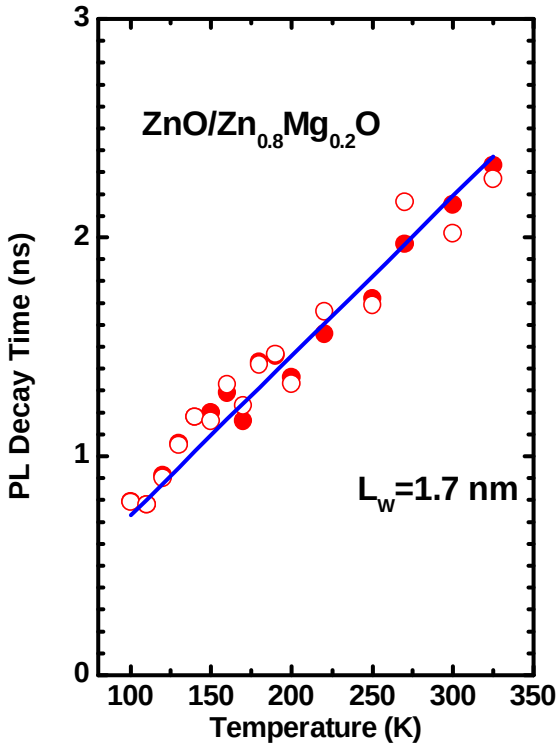

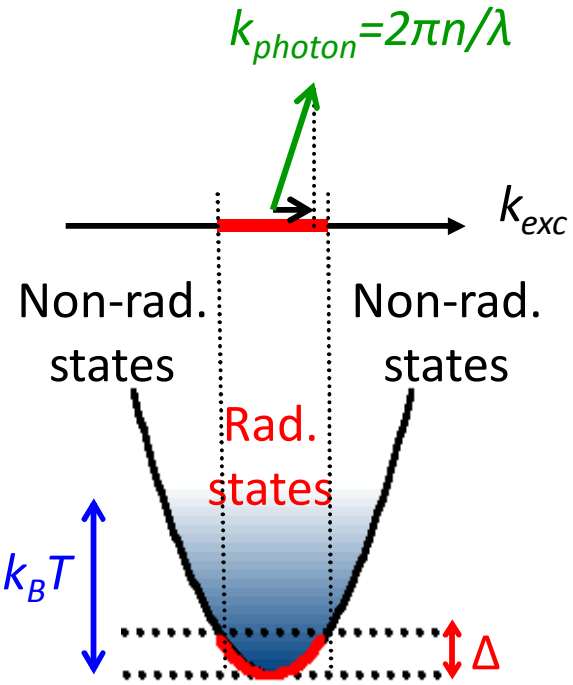

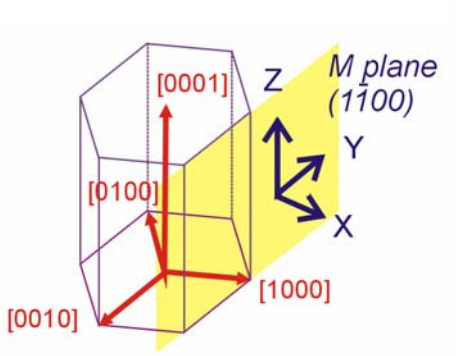

$$\tau_{rad}(T) \approx \frac{2\,c^2\,k_B}{\hbar\,\omega_{LT}\,a_B^3}\left(\frac{1}{m_{ey}+m_{hy}}+\frac{1}{m_{ez}+m_{hz}}\right)^{-1}\frac{\lambda^2}{\omega^3\,l_{eh}^2}\,T$$

• 4- Microcavities , exciton lasing, polariton lasing

Work done under the umbrella of Clermont 4 (director Alexey Kavokin), ANR Zoom (project leader Thierry Guillet) in collaboration with CRHEA, LPN, LASMEA, and EPFL (Th. Guillet, Jesus Zuniga-Perez, Sophie Bouchoule, et al.)

A proposal

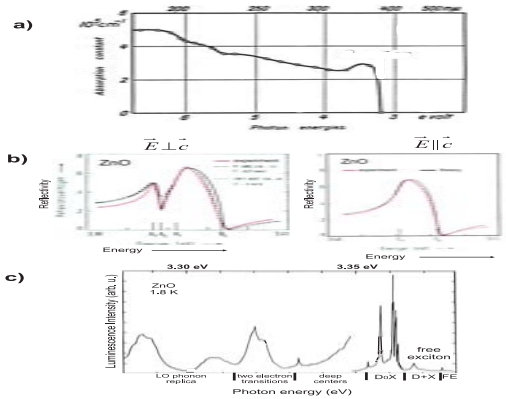

E. Mollwo: Reichsber. Physik **1**, 1 (1943)

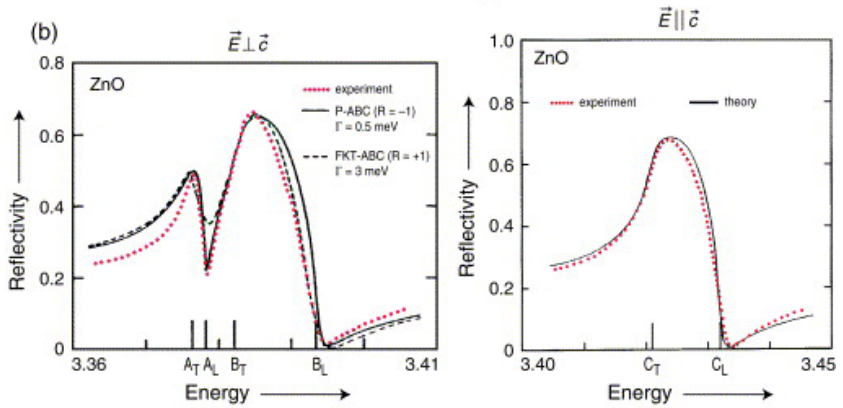

K. Hümmer: Excitonische Polaritonen in einachsigen Kristallen, Habilitation Thesis, Erlangen (1978)

RAPID COMMUNICATIONS

PHYSICAL REVIEW B, VOLUME 65, 161205(R)

ZnO as a material mostly adapted for the realization of room-temperature polariton lasers

Marian Zamfirescu,[1] Alexey Kavokin,[1] Bernard Gil,[2] Guillaume Malpuech,[1,3] and Mikhail Kaliteevski[2]
[1]*LASMEA, UMR 6602 du CNRS, Universit Blaise Pascal–Clermont-Ferrand II, 63177 Aubire Cedex, France*
[2]*GES, CNRS/Universit Montpellier II, Case courrier 074, 34095 Montpellier Cedex 5, France*
[3]*Department of Physics and Astronomy, University of Southampton, Southampton SO17 1BJ, United Kingdom*
(Received 26 November 2001; published 15 April 2002)

Wannier-Mott excitons in the wurzite-type semiconductor material ZnO are stable at room temperature, have an extremely large oscillator strength, and emit blue light. This makes ZnO an excellent potential candidate for the fabrication of room-temperature lasers where the coherent light amplification is ruled by the fascinating mechanism of the Bose condensation of the exciton polaritons. We report the direct optical measurement of the exciton oscillator strength f in ZnO. The longitudinal transverse splitting of the exciton resonances $\Gamma_5(B)$ and $\Gamma_1(C)$ are found to achieve record values of 5 and 7 meV, respectively, that, is two orders of magnitude larger than in GaAs. Second, we propose a model ZnO-based microcavity structure that is found to be the most adapted structure for the observation of the polariton laser effect. We thus can compute the phase diagram of the lasing regimes. A record value of the threshold power of 2 mW per device (at power density of 3000 W/cm^2) at room temperature is found for the model laser structure.

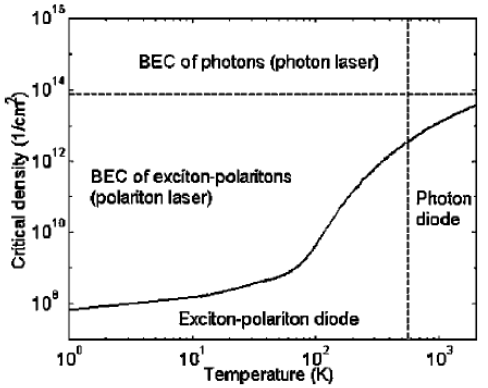

FIG. 4. Exciton-polariton phase diagram in the ZnO microcavity. The solid line shows the polariton critical density versus lattice temperature. The vertical dashed line shows the exciton thermal dissociation limit. The horizontal dashed line shows the Mott transition for excitons.

A comparative study of GaAs, GaN and ZnO

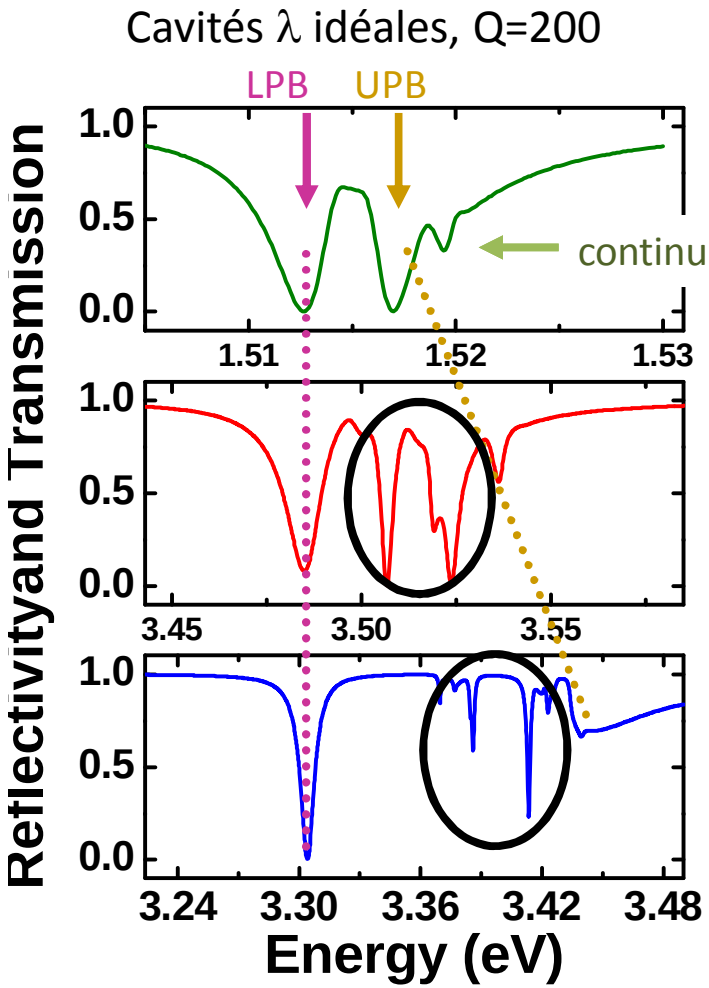

GaAs

$\hbar\Omega_{Rabi} < Ry^*$

GaN

$\hbar\Omega_{Rabi} \cong Ry^* \cong \Delta$

ZnO

$\hbar\Omega_{Rabi} >> Ry^*, \Delta$

In case of GaAs, the Rabi splitting is ~ or smaller than the exciton binding energy.

The GaN case is more complicated thanks to different strong excitonic resonances at energy smaller than the Rabi oscillation splitting energy.

This is reinforced for ZnO for which in addition, absorption by the continuum of states cannot be neglected.

Faure *et al.*, PRB **78**, 235323 (2008)

State of the art at the end of 2009

Data taken from the PhD thesis Stéphane Faure

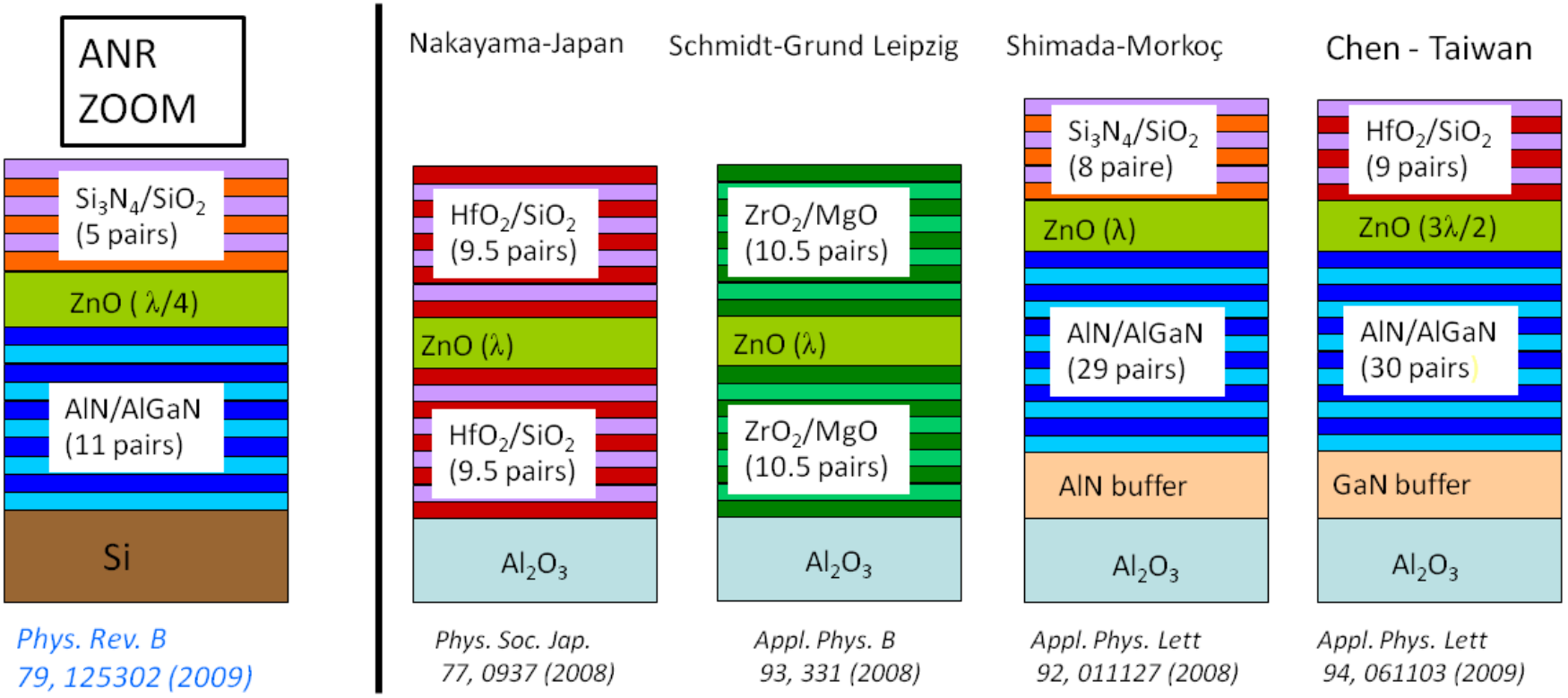

	Phys. Rev. B 79, 125302 (2009)	*Phys. Soc. Jap. 77, 0937 (2008)*	*Appl. Phys. B 93, 331 (2008)*	*Appl. Phys. Lett 92, 011127 (2008)*	*Appl. Phys. Lett 94, 061103 (2009)*
$\hbar\Omega_R$	30 meV 40 meV	80 meV	78 meV 19 meV	50 meV	??
Q	120	500	500	100	220

Exciton lasing in a hybrid ZnO bulk microcavity under large negative detuning conditions

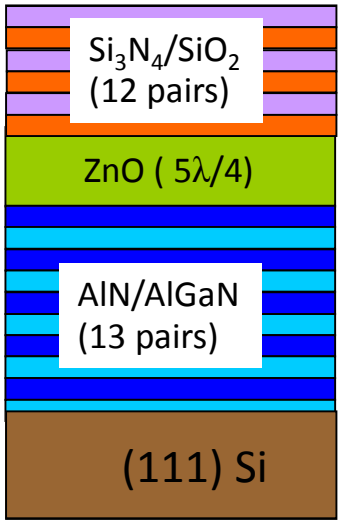

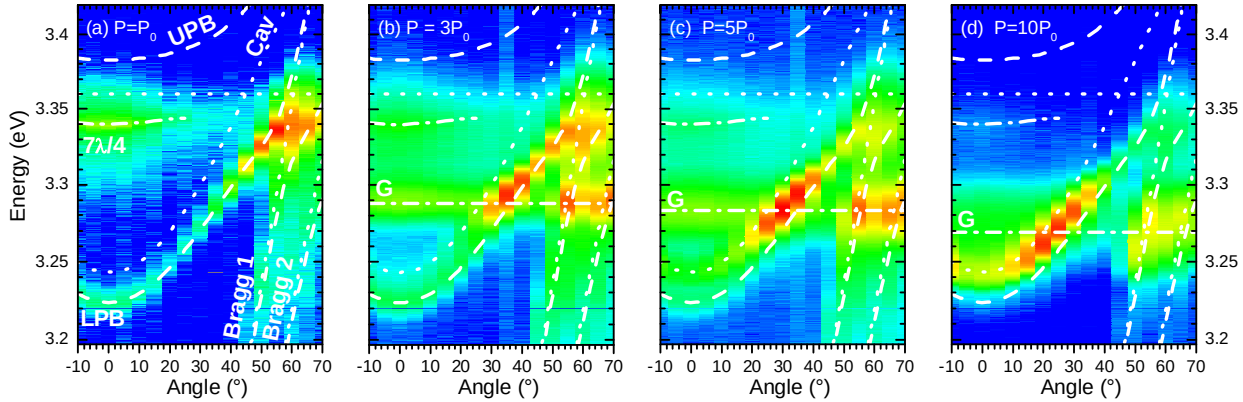

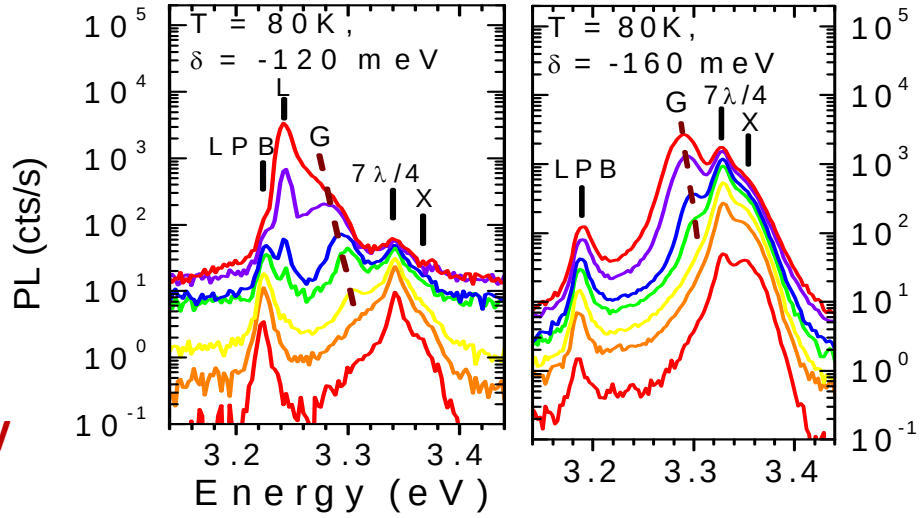

Q = 450

$\hbar\Omega$ = 120 ± 10 meV

δ = -120 to 160 meV

- No photon mode in gain range
- LPB and 7λ/4 still sharp at similar excitation density
- Robust excitons, not EHP : Gain involves excitons
- No 7λ/4 polariton shift,
- small LPB shift : small renormalization

T.Guillet, C.Brimont, P.Valvin, B.Gil, T.Bretagnon, F.Médard, M.Mihailovic, J.Zuniga-Perez, M.Leroux, F.Semond, and S.Bouchoule

Applied Physics Letters, **98** ,211105 (2011)

Polariton lasing in a hybrid ZnO bulk microcavity at 120 K

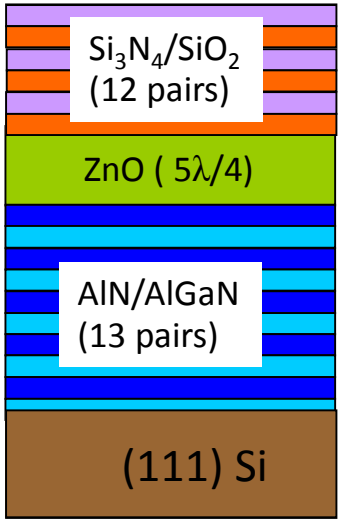

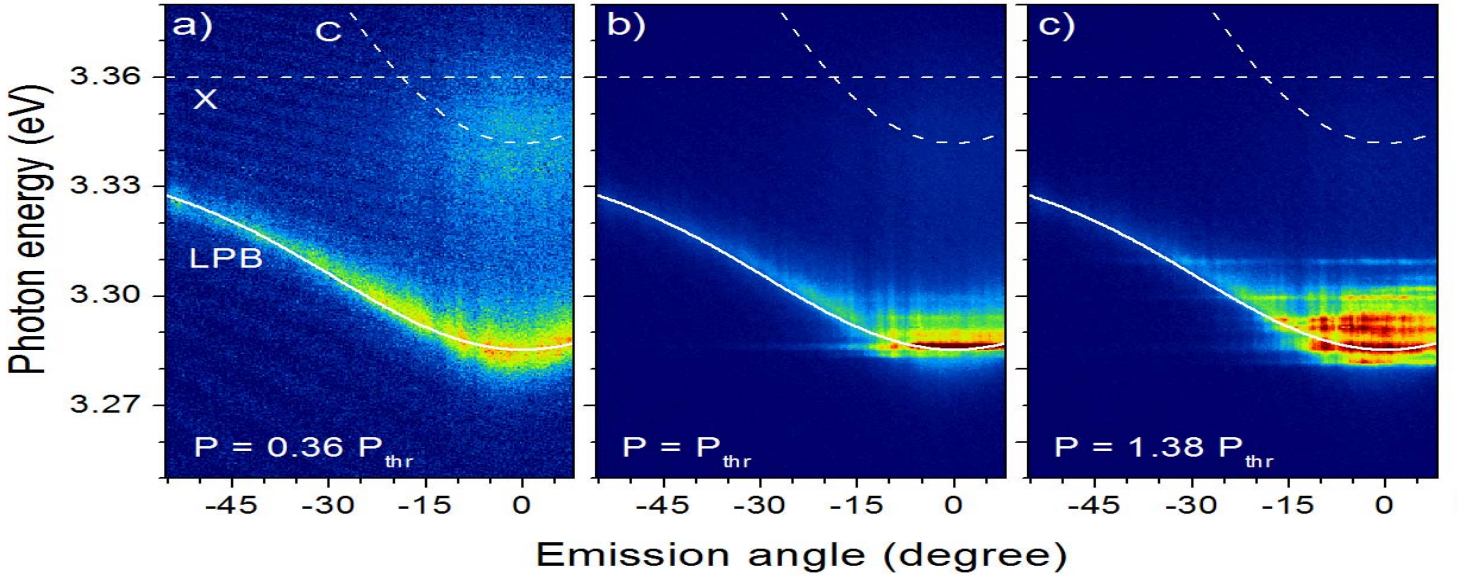

Q = 500

$\hbar\Omega$ = 130 ± 10 meV

δ = -18 ± 5 meV

T. Guillet, M. Mexis, J. Levrat, G. Rossbach, C. Brimont, T. Bretagnon, B. Gil, R. Butté, N. Grandjean, L. Orosz, F. Réveret, J. Leymarie, J. Zúñiga-Pérez, M. Leroux, F. Semond, S. Bouchoule (to appear in APL)

Fresh results from Feng Li

(FL was hired at CRHEA under the context of Clermont 4)

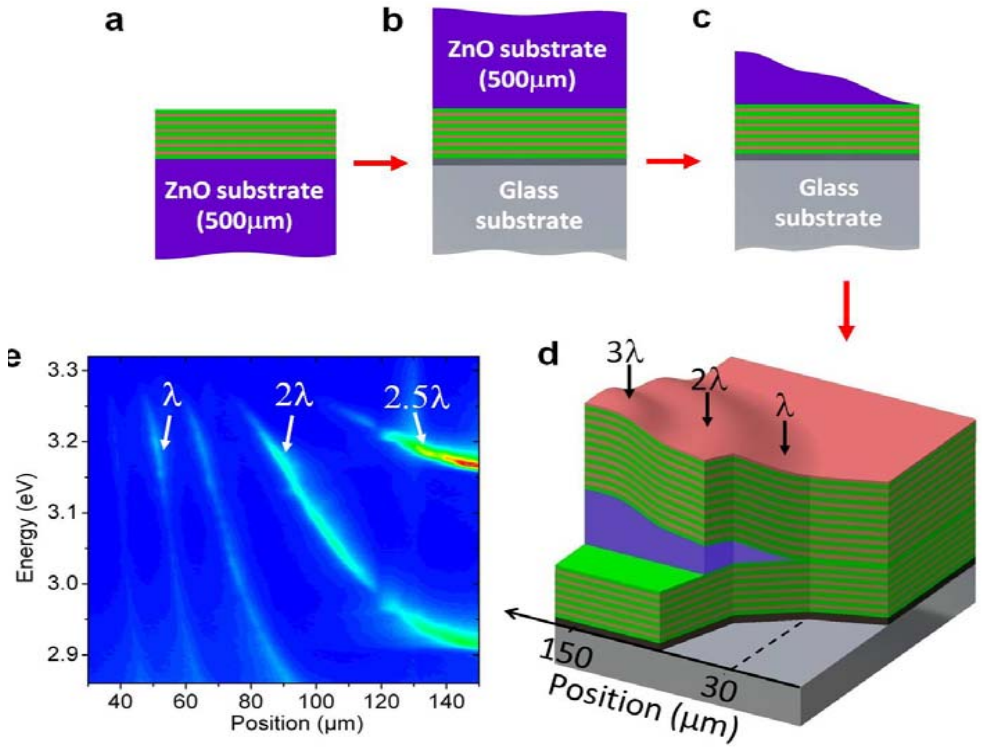

- Double dielectric DBRs → High Q-factor and large stop band.
- ZnO substrate → The best possible bulk ZnO material as the active region.
- Fabrication-induced thickness gradient → allows to access a large range of detunings, enabling the study of polaritons with very different excitonic/photonic fractions.

Borrowed from Feng Li's poster (WEP13)

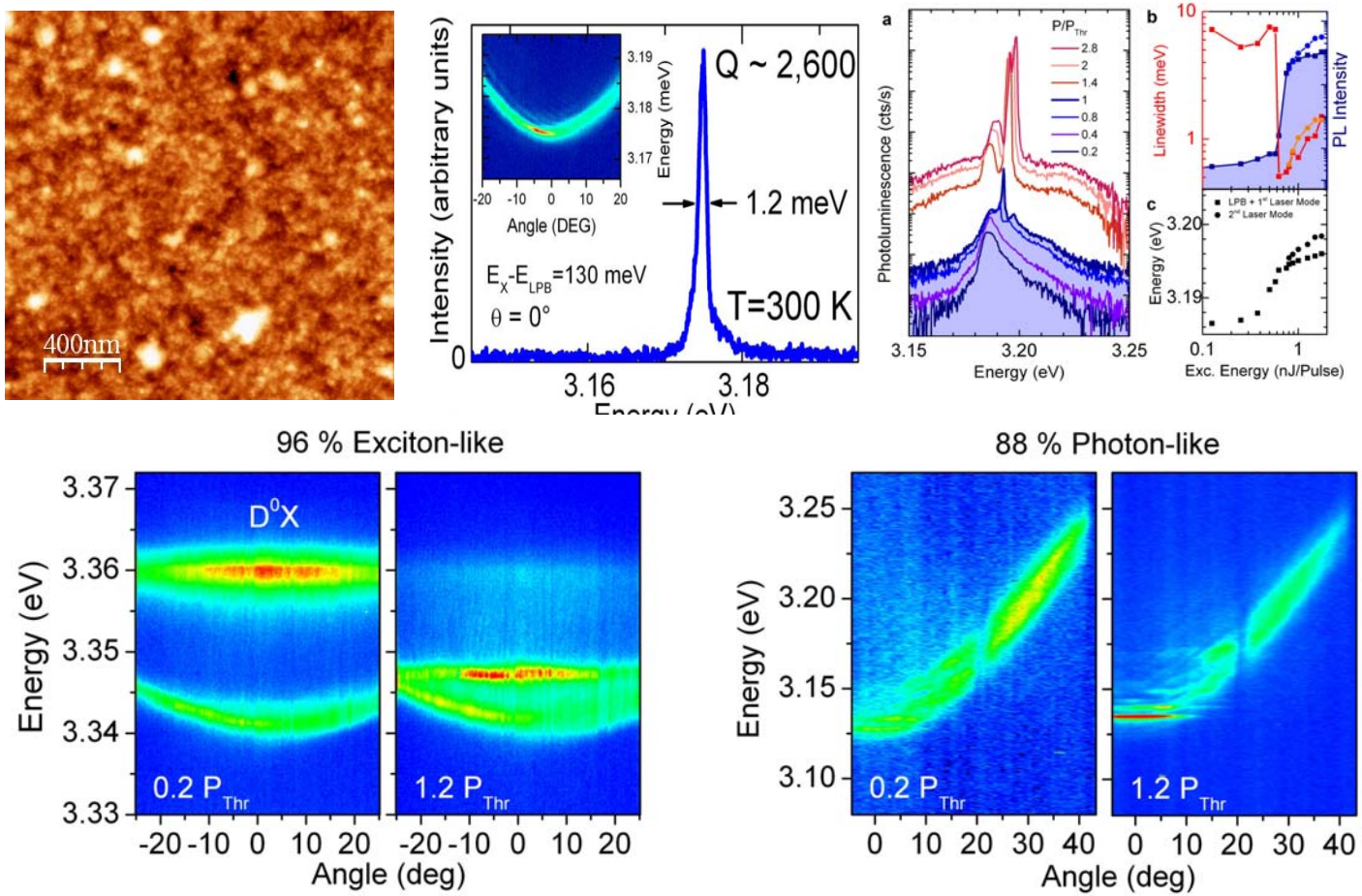

➢Polariton condensate from ~96% exciton-like to 88% photon-like. The optimal detuning at room temperature is close to zero (50% exciton/photon-like).

A complete phase diagram

(Laser threshold vs. offset (E_X-E_{LPB}) & T)

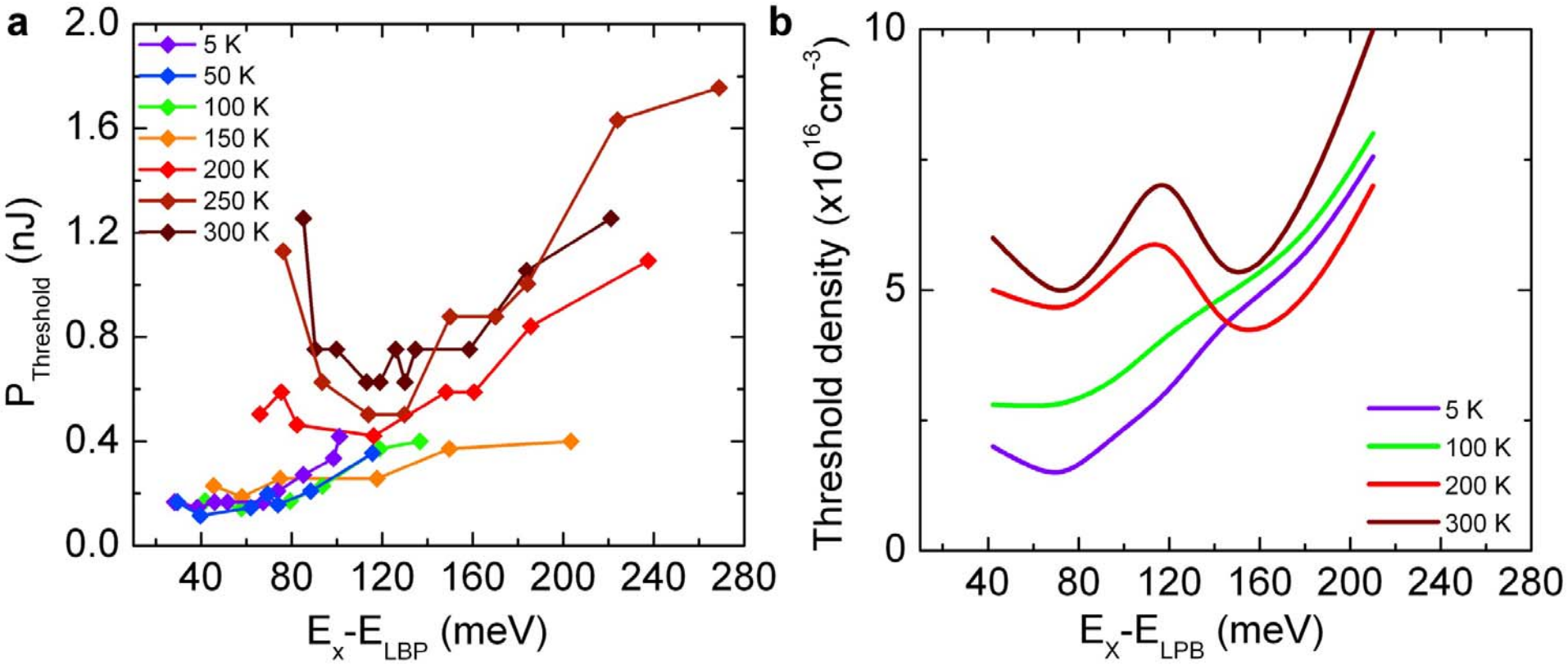

(a). experimental findings

(b) numerical solution of the semiclassical Boltzmann equations (b).

Conclusions

• ZnO-based Quantum Wells have been grown C-plane and M- plane (A- plane too) by molecular beam epitaxy using foreign saphirre substrate of zinc oxide substrate

•These quantum wells exhibit text book optical properties in terms of selection rules for the optical transitions, in terms of defects.

•The homoepitaxial M-plane grown QWs are free from non radiative recombinations up to T = 325 K

•Concerning microcavities, finesses of 500 and Rabi oscillation splitting energies of 120-130 meV are routinely obtained in the context of « CLERMONT 4 » EU and French ANR « ZOOM » research networks.

•Inlarge negative detuning conditions, excitonic gain was demonstrated in such microcavities

•In small negative detuning conditions, polariton lasing was demonstrated up to 300 K

Prospective issues

- a truism: trying to demonstrate p doping, a decent LED and a ridge laser susceptible to challenge nitrides.
- Improving performances of planar microcavities.
- Non polar microcavities.
- photonics using micro disks and WGMs, photonic membranes.
- Nano rods.
- Spin-related phenomena.
-
-

Warm thanks to:

on site: Th. Guillet, Th Bretagnon, C.Brimont, P.Valvin and S.Rousset

Sample growth

- CRHEA – Valbonne

Jean-Yves Duboz

C.Morhain, J.M.Chauveau

Jesús Zúñiga Pérez,

Feng Li

M. Leroux, F. Semond

French ANR project **ZOOM**

European ITN project **Clermont4**

Microcavities

- LPN – Marcoussis

Sophie Bouchoule

- LASMEA – Clermont-Ferrand

Joël Leymarie

F. Médard, P. Disseix, M. Mihailovic

- EPFL – Lausanne

N. Grandjean

J. Levrat, G. Rossbach, R. Butté

Thank you to all my colleagues of Physique des Excitons du Photon et du Spin

Some more…

Piezoelectric and pyroelectric properties of the 32 symmetry classes.

J.F.Nye Physical Properties of Crystal, Oxford University Press, (1957)

32 symmetry classes		
12 non piezo-electric classes		20 piezo-electric classes
O and the 11 centro-symmetric classes	10 non pyroelectric or non polar classes: $D_2, D_{2d}, D_3, D_4, S_4, D_6, C_{3h}, D_{3h}, T, T_d$	10 pyroelectric or polar classes: $C_1, C_2, C_3, C_4, C_6, C_s, C_{2v}, C_{3V}, C_{4V,}$ **C_{6V}**

- Zinc blende crystals are non polar piezo electric crystals
- α -Quartz (D_3) is a non polar piezo electric crystal
- Wurtzite (C_{6v}) crystals are polar piezo electric crystals
- The spontaneous polarization of nitrides is co-linear to the 6-fold axis
- Both magnitude, sign and strength of the piezoelectric polarization can be tuned

The concepts of polar, non polar and semipolar reticular planes

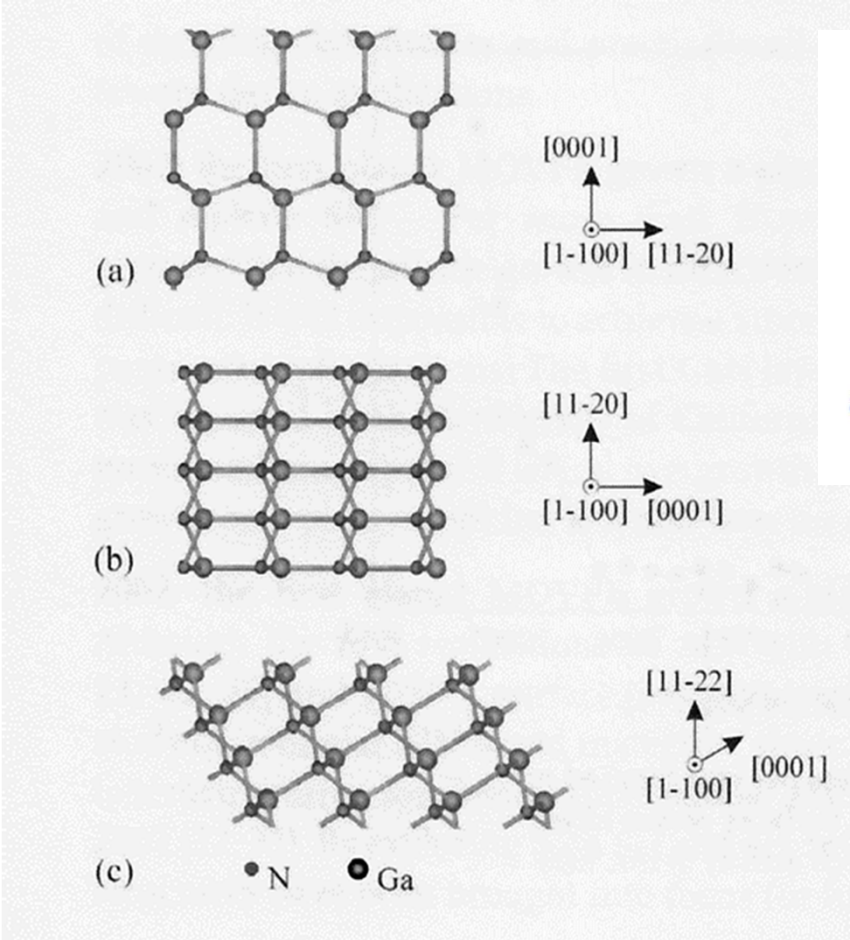

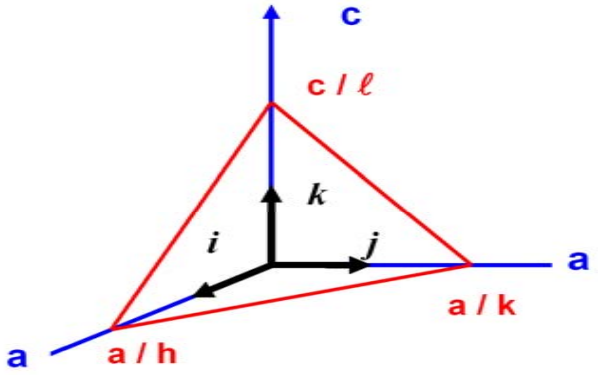

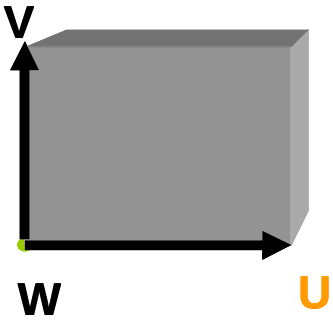

$$\Theta = (W, [001]) = \arccos\left(\frac{1}{\sqrt{1+\frac{4c^2}{3a^2}\frac{(h^2+hk+k^2)}{\ell^2}}}\right)$$

$$P_W = P\cos\Theta$$

Piezo electric effects have to be included

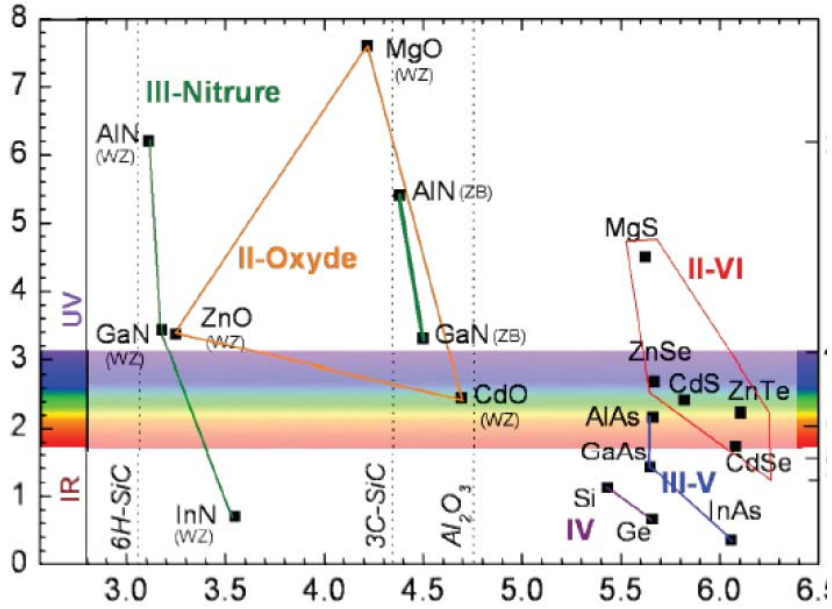

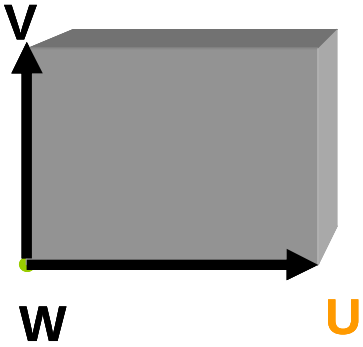

$$\varepsilon_{vv} = \varepsilon_{uw} = \varepsilon_{uv} = 0$$

$$\varepsilon_{uu} = \frac{a - \alpha}{\alpha}$$

$$\varepsilon_{uu} = \frac{B_{\alpha\beta}}{B_{ac}} - 1 = \frac{a\cos(\Theta')}{\alpha\cos(\Theta)} - 1$$

$$\begin{bmatrix} P_x \\ P_y \\ P_z \end{bmatrix} = \begin{pmatrix} 0 & 0 & 0 & 0 & e_{15} & 0 \\ 0 & 0 & 0 & e_{15} & 0 & 0 \\ e_{13} & e_{13} & e_{33} & 0 & 0 & 0 \end{pmatrix} \begin{bmatrix} \varepsilon_{xx} \\ \varepsilon_{yy} \\ \varepsilon_{zz} \\ \varepsilon_{yz} \\ \varepsilon_{xz} \\ \varepsilon_{xy} \end{bmatrix}$$

$$\Omega = C_{12}\sin^2\Theta + C_{13}\cos^2\Theta$$

$$\Xi = (C_{11} + C_{33} - 4C_{44})\cos^2\Theta\sin^2\Theta + (\cos^4\Theta + \sin^4\Theta)C_{13}$$

$$\Phi = C_{11}\sin^4\Theta + (C_{13} + 2C_{44})\,2\cos^2\Theta\sin^2\Theta + C_{33}\cos^4\Theta$$

$$P_{pz} = \cos(\Theta)\left(e_{13} - \left[\{e_{13} + 2e_{15}\}\sin^2(\Theta) + e_{33}\cos^2(\Theta)\right]\frac{\Omega}{\Phi}\right)e_{uu} +$$

$$\cos(\Theta)\left(\left[e_{13}\cos^2(\Theta) + e_{33}\sin^2(\Theta)\right] - \left[e_{13}\sin^2(\Theta) + e_{33}\cos^2(\Theta)\right]\frac{\Xi}{\Phi} - 2e_{15}\sin^2(\Theta)\left[\frac{C_{11}\sin^2(\Theta) + C_{13} + C_{33}\cos^2(\Theta)}{\Phi}\right]\right)e_{vv}$$

« semi polar orientations » cancel QCSE in nitride heterostructures

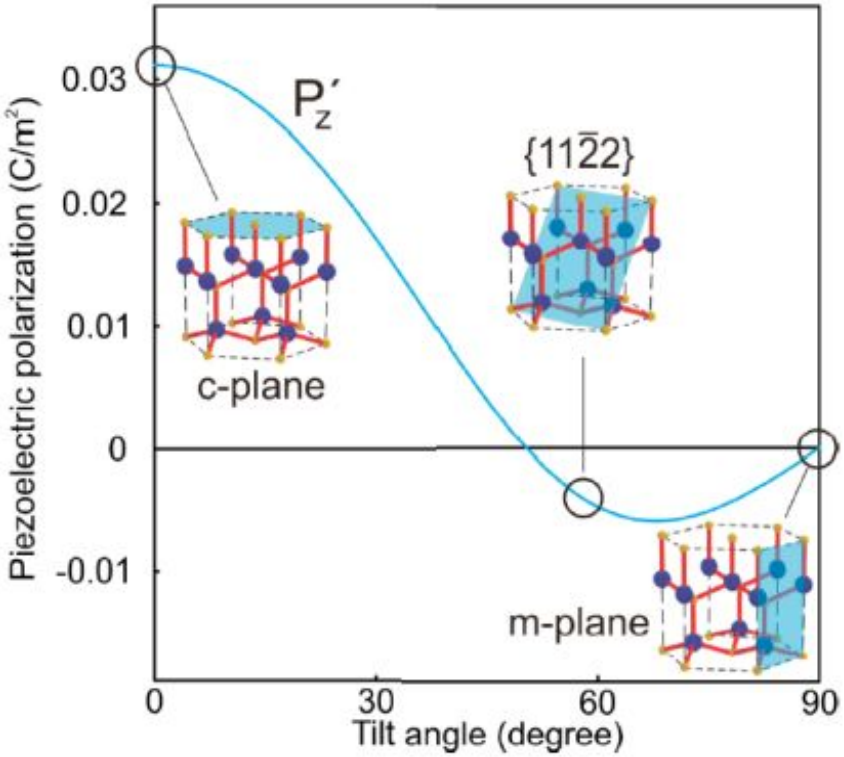

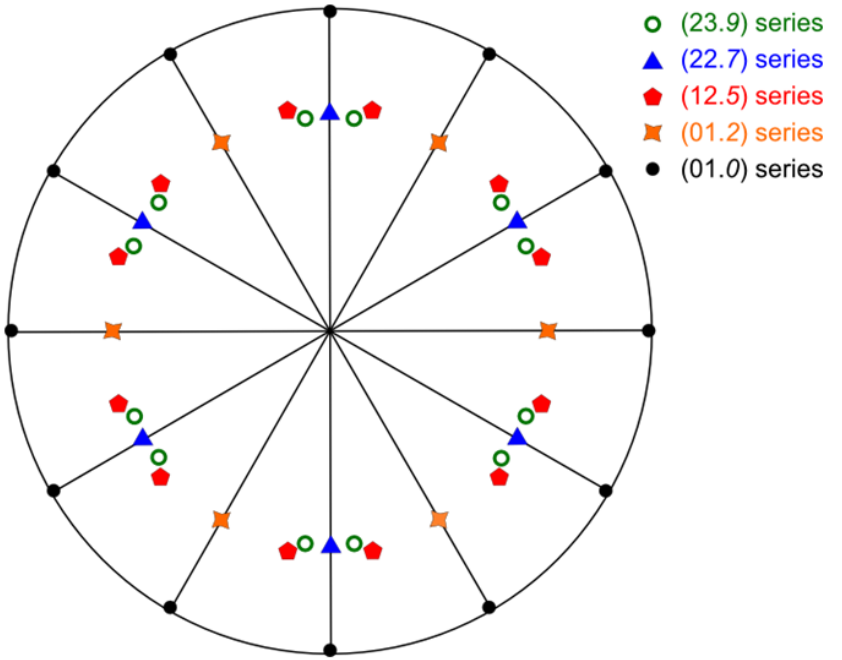

$$\Theta = (W, [001]) = \arccos\left(\frac{1}{\sqrt{1+\frac{4c^2}{3a^2}\frac{(h^2+hk+k^2)}{l^2}}}\right)$$

What about II-VIs?

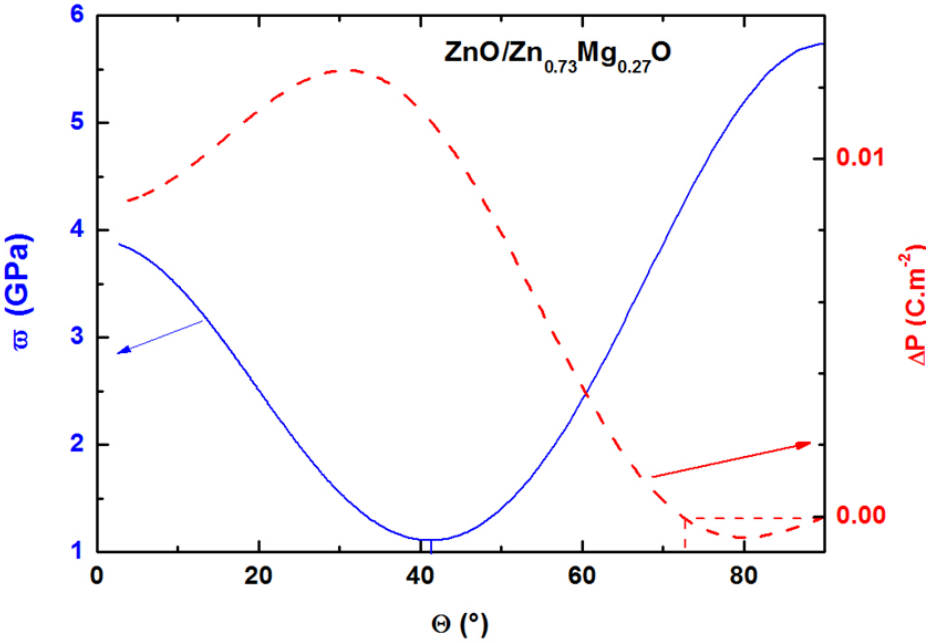

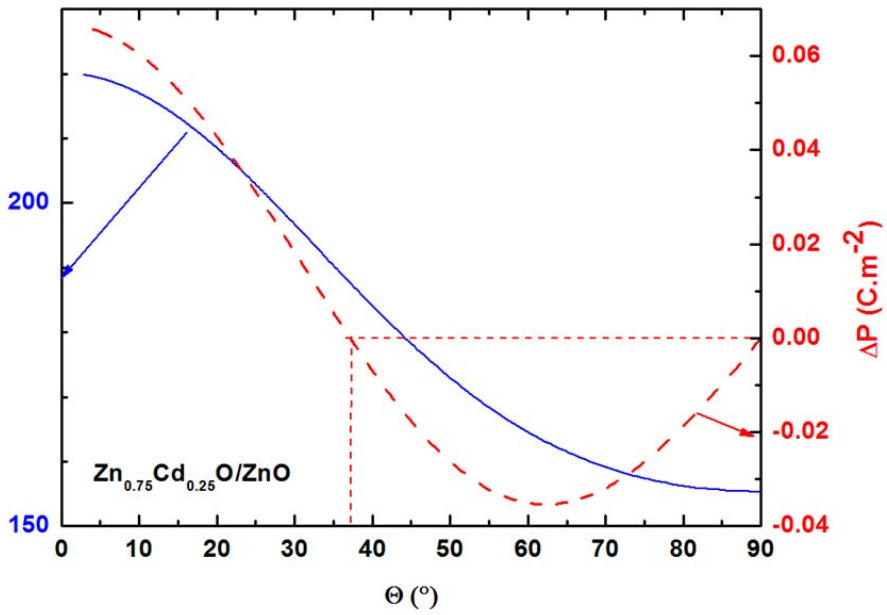

$$\varpi = \frac{1}{2} \sum_{i,j} C_{ij}\, \varepsilon_i\, \varepsilon_j$$